CZECH TECHNICAL UNIVERSITY
IN PRAGUE

Faculty of Electrical Engineering

Department of Telecommunication Engineering

Content Caching in Mobile Networks with UAVs

Diploma Thesis

Study program: Electronics and communications

Field of study: Mobile communications

Supervisor: doc. Ing. Zdeněk Bečvář, Ph.D.

Bc. Filip Krupka

Prague 2023

Declaration

I declare that I have prepared the submitted thesis independently and that I have listed all the information sources used in accordance with the Methodological Instruction on the observance of ethical principles in the preparation of final university theses.

In Prague, January 2023

Bc. Filip Krupka

MASTER'S THESIS ASSIGNMENT

I. Personal and study details

Student's name: **Krupka Filip** Personal ID number: **474243**

Faculty / Institute: **Faculty of Electrical Engineering**

Department / Institute: **Department of Telecommunications Engineering**

Study program: **Electronics and Communications**

Specialisation: **Mobile Communications**

II. Master's thesis details

Master's thesis title in English:

Content Caching in Mobile Networks with UAVs

Master's thesis title in Czech:

Kešování informačního obsahu v mobilních sítích s létajícími základnovými stanicemi

Guidelines:

Study the concept of popular content caching at the edge of mobile network with UAVs serving as base stations.Propose an algorithm for energy efficient delivery of the popular content changes in the flying base stations to the users. To this end, consider optimization of communication parameters and/or positions of flying base stations in real time so that the low energy consumption is ensured together with a low delay in delivery of the content to the users. Evaluate performance of the proposed algorithmic simulations and compare it with related works.

Bibliography / sources:

[1] M. Zhang, M. El-Hajjar, S. Xin Ng, "Intelligent Caching in UAV-Aided Networks," IEEE Transactions on Vehicular Technology, vol. 71, no. 1, January 2022.
[2] A.A. Khuwaja, Y. Zhu, G. Zheng, Y. Chen, W. Liu, "Performance Analysis of Hybrid UAV Networks for Probabilistic Content Caching," IEEE Systems Journal, vol. 15, no. 3, Sept. 2021.
[3] J. Ji, K. Zhu, D. Niyato, R. Wang, "Joint Cache Placement, Flight Trajectory, and Transmission Power Optimization for Multi-UAV Assisted Wireless Networks," IEEE Transactions on Wireless Communications, vol. 19, no. 8, Aug. 2020.
[4] J. Yang, S. Xiao, B. Jiang, H. Song, S. Khan, and S. ul Islam, "Cache-Enabled Unmanned Aerial Vehicles for Cooperative Cognitive Radio Networks," IEEE Wireless Communications, April 2020.

Name and workplace of master's thesis supervisor:

doc. Ing. Zdeněk Bečvář, Ph.D. Department of Telecommunications Engineering FEE

Name and workplace of second master's thesis supervisor or consultant:

Date of master's thesis assignment: **14.09.2022** Deadline for master's thesis submission: **10.01.2023**

Assignment valid until: **19.02.2024**

doc. Ing. Zdeněk Bečvář, Ph.D. Supervisor's signature	Head of department's signature	prof. Mgr. Petr Páta, Ph.D. Dean's signature

III. Assignment receipt

The student acknowledges that the master's thesis is an individual work. The student must produce his thesis without the assistance of others, with the exception of provided consultations. Within the master's thesis, the author must state the names of consultants and include a list of references.

.	
Date of assignment receipt	Student's signature

Abstract

Mobile networks with integrated content caching and unmanned aerial vehicles (UAVs) serving as flying base stations (FlyBSs) are capable of improved distribution of popular content to user equipments (UEs) compared to a common mobile network. The use of FlyBSs in cache-enabled networks has already been investigated in multiple related works. However, the majority of these works focus on the throughput and reduction of the content delivery delay, but the energy consumed for communication is not reflected. Thus, to address the energy consumed for communication in UAV-assisted mobile networks with content caching, this thesis proposes a novel energy-efficient association of UEs to base stations (BSs), transmission power navigated positioning of FlyBSs, and content delivery through multi-hop relaying with FlyBSs repositioning. Simulation results show the energy consumed for communication decreases by 27%-66% with respect to related works. The gain depends on the number of FlyBSs and UEs in the network and on the size of cache storage on FlyBSs. The delivery delay is then, in comparison with related works, improved by 26%-58%.

Index terms

Mobile network, content caching, unmanned aerial vehicle, energy consumption, transmission power, data transmission, communication capacity

Abstrakt

Mobilní sítě s integrovaným kešováním obsahu a s bezpilotními vzdušnými letouny (UAVs) sloužícími jako létající základnové stanice (FlyBSs) jsou schopny lepší distribuce populárního obsahu mezi uživatelskými zařízeními (UEs) než běžné mobilní sítě. Použití FlyBSs v sítích s integrovaným kešováním je již adresováno v mnoha souvisejících pracích. Většina těchto prací se však zaměřuje na propustnost sítě a snížení zpoždění doručení obsahu, ale energie spotřebovaná na komunikaci není uvažována. Pro řešení energie spotřebované pro komunikaci v mobilních sítích využívajících FlyBSs a kešování obsahu, tato práce navrhuje nové techniky energeticky efektivní asociace UEs se základnovými stanicemi (BSs), výkonově výhodného určení pozice FlyBSs, a techniku doručení obsahu za použití multi-hop přeposíláni obsahu s eventuálním přemísťováním FlyBSs. Výsledky simulace ukazují energie spotřebovaná na komunikaci je snížena o 27% - 66% ve srovnání se souvisejícími pracemi. Hodnota poklesu záleží na počtu FlyBSs a UEs v mobilní síti a na velikosti kešovací paměti na FlyBSs. Zpoždění doručení obsahu je pak, vůči souvisejícím pracem snížené o 26% - 58 %.

Klíčová slova

Mobilní síť, kešování obsahu, bezpilotní vzdušný letoun, spotřeba energie, vysílací výkon, přenos dat, komunikační kapacita

Acknowledgment

I would like to express my gratitude to doc. Ing. Zdeněk Bečvář, Ph.D. for the supervision, for keeping me in the right direction, and for the valuable advice given during the work on the diploma thesis. I would also like to thank my family for their support during my academic career.

Contents

List of Figures

List of Tables

List of Abbreviations

UAV	Unmanned Aerial Vehicle
BS	Base Station
SBS	Static Base Station
FlyBS	Flying Base Station
UE	User Equipment
FSPL	Free Space Path Loss
OFDMA	Orthogonal Frequency Division Multiple Access
LOS	Line of Sight
NLOS	Non-line of Sight
SINR	Signal to Interference and Noise Ratio
MEC	Mobile Edge Computation
WPT	Wireless Power Transfer

1 Introduction

One of the developments of wireless mobile networks that are expected to be included in future mobile networks includes unmanned aerial vehicles (UAVs) as flying base stations (FlyBSs). The integration of UAVs as FlyBSs in mobile networks and their advantages are described in [1]. The FlyBSs can be used for the purposes of an increase in the capacity of the mobile network in high-density areas with a temporary heavy load [2]. The paper [2] characterizes the use of FlyBSs in hotspot areas like sports or music events where a high number of user equipments (UEs) groups in a small area. FlyBSs increase the flexibility of the infrastructure and enable the mobile network to be established in areas where it would not be possible with conventional static base stations (SBSs). The paper [3] proposes the use of UAVs in emergency scenarios where the FlyBSs relay the communication of UEs in locations unreachable by the static infrastructure.

The relaying in UAV-assisted mobile networks is significantly beneficial in scenarios where the direct connection between UEs and SBSs is inefficient due to the distance or blockage, and the connection can be established via relaying with better channel quality. The paper [4] presents the basic model of a UAV-assisted mobile relaying system, emphasizing throughput maximization. The relaying is further investigated in [5], where the joint optimization of the UAV's trajectory and transmission power was proposed to achieve minimization of outage probability of the UAV-assisted mobile relay network. The paper [6] then proposes the joint optimization of UAV trajectory and time scheduling to guarantee secure transmission in UAV-relaying systems with local caching. The maximization of the reliability of the UAV-assisted network by optimal placement of UAVs is proposed in [7]. The FlyBSs can also be used for computational purposes, as presented in [8], offering mobile edge computation (MEC) resources to UEs to enable offloading of the computational tasks to FlyBSs or SBSs in the mobile network. The paper [9] then describes MEC as one of the key technologies in future 5G networks.

An essential aspect of mobile networks in the days to come is storing contents close to UEs, known as content caching. The repeated downloads of identical content by multiple UEs from distant servers burden communication resources significantly. Content caching in mobile networks reduces the number of downloads of the same content, frees up

communication resources, and reduces the power consumption of the whole mobile network [10]. The caching of contents close to the UEs includes the decision mechanisms of choosing the contents for caching. The paper [11] investigates the deployment of caching in mobile networks and the most beneficial caching strategy for various mobile network architectures. The paper [12] then evaluates the efficiency of content placement by evaluating capacity and energy efficiency. The paper [13] then exploits the high mobility of cache-enabled FlyBSs to maximize the minimum throughput in the network. Then, the paper [14] describes the caching on FlyBSs of selected parts of contents, and the content is delivered from multiple FlyBSs. This work also investigates the use of wireless power transfer (WPT), allowing the transfer of power to the FlyBSs wirelessly, alleviating the problem of a limited battery of UAVs.

Energy consumption is crucial for UAV-assisted mobile networks containing caching [15]. For this reason, the energy consumed for communication in the network involving FlyBSs in its architecture is the main objective investigated in this thesis. In contrast to the above-mentioned related works, this thesis introduces mechanisms for UAV-assisted mobile networks with content caching designed to decrease the energy consumed for communication. The contributions of this work are summarized as follows:

- Proposed is a delivery of contents through multi-hop relaying using the connections between FlyBSs and the SBS and between the FlyBSs themselves. This technique significantly decreases the total transmission power needed for content delivery over long distances.
- The decrease in energy consumed for communication also supports the introduction of the movement of FlyBSs, which reflects the low transmission power needed for content delivery, and the introduction of FlyBS repositioning towards UEs requesting the content in prespecified situations.
- Above mentioned mechanisms are supported by the UE to base station (BS) association considering both transmission power and channel capacity of the content delivery. The mechanisms then significantly improve the energy consumed for communication in the mobile network and free up communication resources.
- Via simulation demonstrates that implementing proposed mechanisms in UAV-assisted mobile networks with content caching decreases the energy consumed for communication by up to 66%.

The structure of the thesis is as follows. The next chapter introduces the main principles of mobile networks and the variables used in this thesis. Then, in Chapter 3 are proposed mechanisms for UAV-assisted mobile networks containing content caching supposed to decrease the energy consumed for communication in the mobile network. Chapter 4 describes the mobile network simulation with implemented proposed mechanisms and presents the simulation results for simulated parameters compared with related works. Chapter 5 then concludes the thesis and summarizes the contribution of this work.

2 System model and problem formulation

This Chapter covers the main characteristics of the wireless communication network. First, models related to the network, including types of BSs, UEs, their behavior, and deployment, are presented. Then, the channel and interference model characterizing the propagation between BSs, UAVs, and UEs in the network is described. Last, the model of caching is introduced.

2.1 Network modeling

The network topology is a three-tier wireless mobile network with N BSs composed of one SBS and U UAVs serving as FlyBSs. The BSs are defined by the set $\boldsymbol{N} = \{n_1, n_2, \dots, n_N\}$ and FlyBSs are defined by the set $\boldsymbol{U} = \{u_1, u_2 \dots, u_U\}$. Each BS is equipped with a single antenna with a specified gain G [15]. The wireless network operates in the restricted area consisting of K UEs defined by the set $\boldsymbol{K} = \{k_1, k_2, \dots, k_K\}$.

The UEs and FlyBSs move in the restricted area in the x, y, and z coordinates. Each UE continuously moves in the restricted area in a randomized direction with a maximum velocity of $V_{max}^{(UE)}$ [11]. The x and y coordinates of the UEs are present in the sets $\boldsymbol{R}^{(\boldsymbol{x},\boldsymbol{UE})} = \left\{x_1^{(UE)}, \dots, x_K^{(UE)}\right\}$ and $\boldsymbol{R}^{(\boldsymbol{y},\boldsymbol{UE})} = \left\{y_1^{(UE)}, \dots, y_K^{(UE)}\right\}$, and the set $\boldsymbol{R}^{(\boldsymbol{UE})} = \left\{r_1^{(UE)}, \dots, r_K^{(UE)}\right\}$ then defines the positions of the UEs in the network, where $r_k^{(UE)}$ represents the position of the UE k. UEs move on a flat surface; thus, the z coordinate is for each UE neglected. FlyBSs move in the restricted area above the UEs in the altitude h, which represents the z coordinate, with maximum velocity $V_{max}^{(FlyBS)}$ for horizontal directions and $V_{max}^{(FlyBS,h)}$ for the vertical direction [11][16]. The x and y coordinates of FlyBSs are present in the sets $\boldsymbol{R}^{(\boldsymbol{x},\boldsymbol{FlyBS})} = \left\{x_1^{(FlyBS)}, \dots, x_U^{(FlyBS)}\right\}$ and $\boldsymbol{R}^{(\boldsymbol{y},\boldsymbol{FlyBS})} = \left\{y_1^{(FlyBS)}, \dots, y_U^{(FlyBS)}\right\}$, and the positions of FlyBSs in the network are then defined by the set $\boldsymbol{R}^{(\boldsymbol{FlyBS})} = \left\{r_1^{(FlyBS)}, \dots, r_U^{(FlyBS)}\right\}$[3].

The UEs in the restricted area are divided into several groups, where each group is served by one BS. Thus, the number of groups equals the number of BSs in the area. Then the BS

n serves to the $\Upsilon_n = \{k_{n,1}, .., k_{n,m_n}, \dots, k_{n,M_n}\}$ set of UEs, where M_n is the number of UEs in the group served by the BS n [11][15]. The set $\boldsymbol{a_n^{(UE)}} = \{a_{n,1}^{(UE)}, \dots, a_{n,k}^{(UE)}, \dots, a_{n,K}^{(UE)}\}$ defines the associations between the BSs and the UEs, where:

$$a_{n,k}^{(UE)} = \begin{cases} 1, & \text{if the UE } k \text{ is associated with the BS } n, \\ 0, & \text{otherwise.} \end{cases} \tag{2.1}$$

The set $\boldsymbol{a_n^{(BS)}} = \left\{a_{n,1}^{(BS)}, \dots, a_{n,j_n}^{(BS)}, \dots, a_{n,J_n}^{(BS)}\right\}$ then defines the associations between the BSs, where the BS j_n is the neighboring BS to the BS n. The association between the BSs is established when the transmission between the BSs is requested [3]. Associations then follow:

$$a_{n,j_n}^{(BS)} = \begin{cases} 1, & \text{if the BS } n \text{ transmits data to the BS } j_n, \\ 0, & \text{otherwise.} \end{cases} \tag{2.2}$$

The association sets are then composed in matrix $\boldsymbol{A} = \left\{\boldsymbol{a_1^{(UE)}}, \dots, \boldsymbol{a_N^{(UE)}}, \boldsymbol{a_1^{(BS)}}, \dots, \boldsymbol{a_N^{(BS)}}\right\}$ of associations in the network [3]. The association mechanism of UEs to BSs is described in Chapter 3.1. The FlyBSs are then moving according to the movement of the UEs, as described in Chapter 3.2. The system model is illustrated in Figure 2.1.

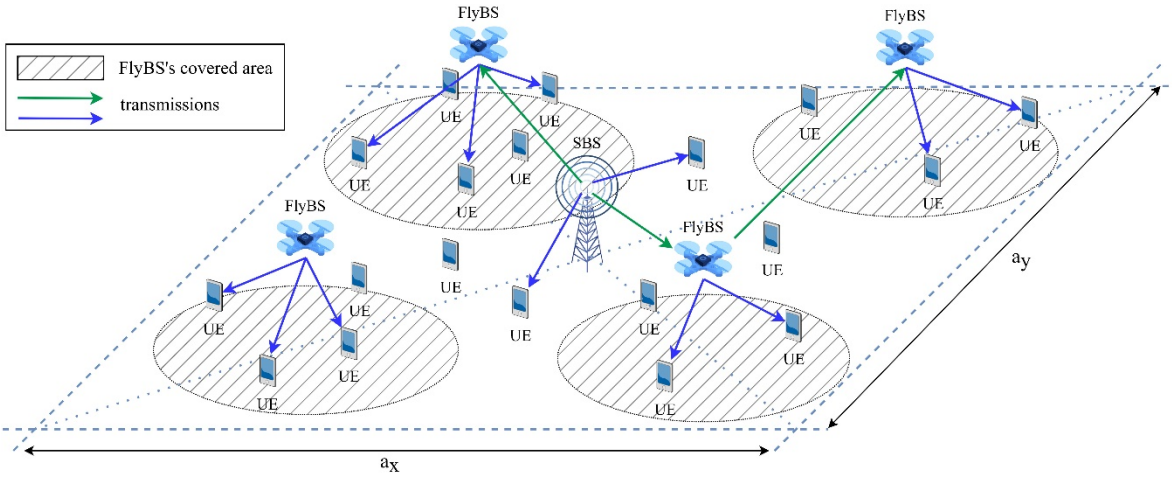

Figure 2.1 - Illustration of the communication network in the restricted area

The operating altitude h_s of the SBS is unchangeable, but the operating altitude of FlyBSs changes over time. The operating altitude h_u of the FlyBS u from the set $\boldsymbol{U}$ is determined according to the formula:

$$h_u = \frac{\max(\boldsymbol{d_u^{(UE)}})}{tg(\alpha)} \geq h_{min}\,, \tag{2.3}$$

where α represents the angle of half of the FlyBS antenna's coverage [16]. The angle α is demonstrated in Figure 2.2. $\boldsymbol{d_u^{(UE)}} = \left\{d_{u,1}^{(UE)}, \dots, d_{u,M_u}^{(UE)}\right\}$ then represents the set of horizontal distances between the serving FlyBS u and M_u UEs included in the group served by the selected FlyBS u. Thus, the operating altitude of the FlyBS u is influenced by the angle of the FlyBS antenna's coverage and by the UE in the group of the FlyBS u, whose horizontal distance from the FlyBS u is the highest. This distance afterward represents the radius of the FlyBSs' covered area. The operating altitude is then limited from the bottom by constant h_{min} [16]. The actual altitudes of all FlyBSs in the network are present in the set $\boldsymbol{R^{(h,FlyBS)}} = \{h_1, \dots, h_U\}$.

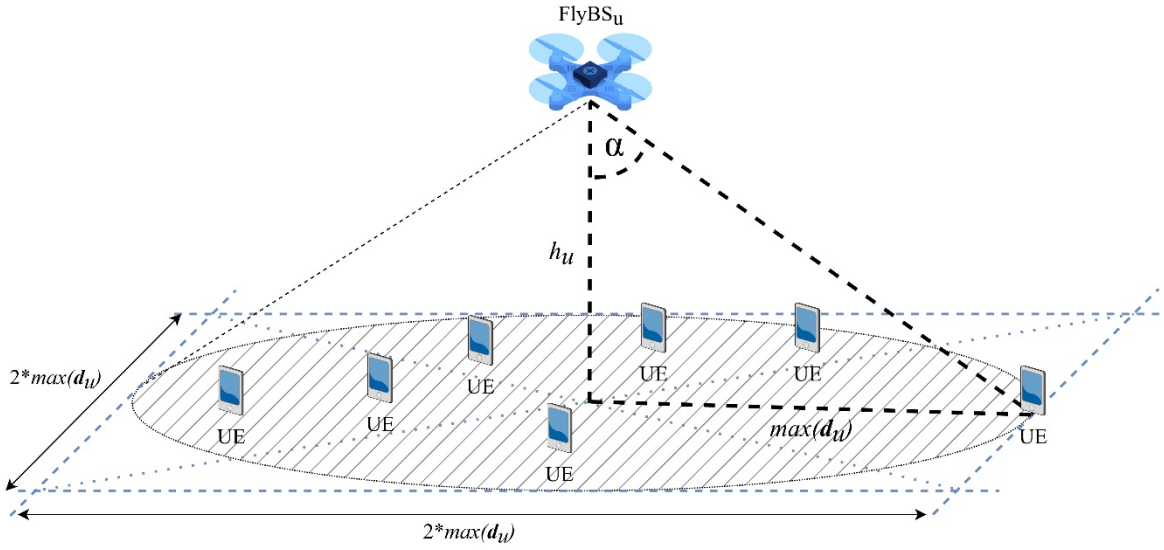

Figure 2.2 - The FlyBS's coverage

2.2 Channel model

For communication between BSs and UEs, the same as for communication between BSs themselves, the signal level is evaluated according to the Free Space Path Loss (FSPL) model. The FSPL would be in the case of the Non-line-of-sight (NLOS) environment affected by the objects in the path of connection [12][15]. For purposes of simplification, only Line-of-sight (LOS) communication is considered. The channel gain describes the difference in the signal level between the transmitter and receiver of the connection.

The channel gain is based on the FSPL model and is described as:

$$g = \left(\frac{c}{4\pi D f}\right)^2, \tag{2.4}$$

where constant c represents the speed of light, variable f represents the carrier frequency, and variable D represents the communication distance, which is defined as the Euclidian distance between the transmitter and receiver of the channel [3][11].

The antenna gain in the communication between UEs and BSs enhances the channel gain. The channel gain of the connection between the BS n and the UE k is then described as:

$$g_{n,k}^{(UE)} = \left(\frac{c}{4\pi D_{n,k}^{(UE)} f}\right)^2 * G_n, \tag{2.5}$$

where $D_{n,k}^{(UE)}$ is the communication distance between the BS n and the UE k present in the set $\boldsymbol{D_n^{(UE)}} = \left\{D_{n,1}^{(UE)}, \dots, D_{n,K}^{(UE)}\right\}$ [3]. Variable G_n is then the gain of the antenna of the BS n. The gain of the UE's antenna is minimal, so it is neglected in the calculation. In the case of the connection between the BS n and the BS j_n, the channel gain of the connection is described as:

$$g_{n,j_n}^{(BS)} = \left(\frac{c}{4\pi D_{n,j_n}^{(BS)} f}\right)^2 * G_n * G_{j_n}, \tag{2.6}$$

where $D_{n,j_n}^{(BS)}$ represents the distance between the BS n and the BS j_n present in the set $\boldsymbol{D_n^{(BS)}} = \left\{D_{n,1}^{(BS)}, \dots, D_{n,J_n}^{(BS)}\right\}$ of communication distances between the BS n and its neighboring. Variable G_{j_n} then represents the antenna gain of the neighboring BS j_n [3].

To ensure a high signal level for each channel, the guaranteed received power $p^{(rx)}$ is set in the network. The transmission power allocated on the BS for the transmission of contents is then described according to the formula:

$$p^{(tx)} = \frac{p^{(rx)}}{g}. \tag{2.7}$$

The formula presents that with the guaranteed received power $p^{(rx)}$, the transmission power is directly dependent on the channel gain. It then relies on the communication distance, the

same as on the antenna gains of the transmitter and receiver [11]. The transmission powers allocated for the content delivery to each UE, regardless of the transmitting BS, are the same as the transmission powers allocated for content delivery to BSs defined by the set $\boldsymbol{P} = \left\{p_1^{(tx)}, \dots, p_K^{(tx)}, p_1^{(tx,BS)}, \dots, p_N^{(tx,BS)}\right\}$[3].

The energy consumption of each BS is determined as the power spent during a period. The energy consumption would be composed of transmission powers allocated by the BS for the content delivery and propulsion power consumed for the operation of the UAV [15][18]. Since this thesis aims to decrease the energy consumption caused by the transmission power in UE-directed communication, the propulsion power is neglected, and the parameter is the energy consumed for communication. The power allocated for caching by the SBS is also not included in the calculation of energy consumed for communication, as it is a backhaul mechanism that uses different communication resources and does not influence the UE-directed communication in the proposed network. Then, the energy consumed for communication by the BS n in Wh for the chosen period T in seconds is formulated as:

$$E_n = \frac{1}{3600} * \int_1^T \left(\sum_k^K p_{n,k,t}^{(tx)} + \sum_{j_n}^{J_n} p_{n,j_n,t}^{(tx)} \right) dt \tag{2.8}$$

where $p_{n,k,t}^{(tx)}$ represents the transmission power allocated by the BS n for transmission of content to the UE k in time t, and $p_{n,j,t}^{(tx)}$ represents the transmission power allocated by the BS n in time t for transmission of content to the neighboring BS j_n [18][19].

The wireless communication runs on the carrier frequency *f,* and the exact size of the bandwidth B awards each BS. In the network, orthogonal frequency division multiplexing (OFDMA) is implemented, so the bandwidth B is distributed by each BS equally between channels to active UEs in its group and between established channels with the neighboring BSs. Active UEs are UEs currently requesting content. Thus, the bandwidth available on the BS n for one channel is given accordingly:

$$B_n = \frac{B}{M_n^{(active)} + H_n}, \tag{2.9}$$

where $M_n^{(active)}$ represents the number of UEs requesting content connected to the BS n, and H_n represents the number of established channels between the BS n and the neighboring BSs [3][5].

The channel between a BS and a UE might be established as one direct link or relay link. The relay link comprises one backhaul link from the source BS to a relay BS and one access link between the relay BS and the UE. This relay link is illustrated in Figure 2.3.

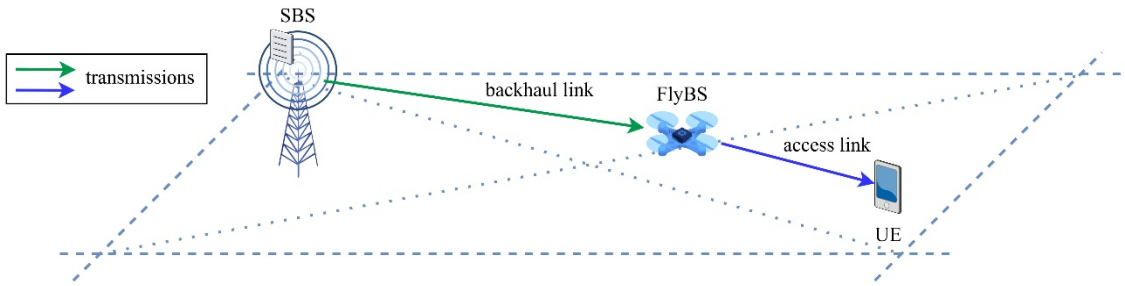

Figure 2.3 - Relay link with one relay BS

Each channel is affected by interference from the surrounding environment and by noise. The interference is caused by the communication of neighboring BSs that use different or the same spectral resources. The interference by BSs using the same spectral resources applies only to the access link in the relay link [3][20]. The Thermal noise then represents the noise. The quality of each channel is represented by the signal-to-interference-plus-noise ratio (SINR), which is for the direct connection between the BS n and the UE k described as:

$$SINR_{n,k}^{(D)} = \frac{p_{n,k}^{(rx)}}{B_n\sigma + \sum_{w_k} p_{w_k}^{(tx)} g_{w_k,k}}, \tag{2.10}$$

where σ represents the noise spectral density. Variable $p_{w_k}^{(tx)}$ represents the transmission power of the interfering neighboring BS w_k from the set $\boldsymbol{N_k^{(int)}} = \{\boldsymbol{n}_1, \dots, \boldsymbol{n}_{W_k}\}$ of interference sources to the UE k using different spectral resources than the BS n. The $g_{w_k,k}$ then represents the propagation channel gain between the interfering BS w_k and the UE k [15][20][21].

In the case of a relay link between the BS n and the UE k, containing the BS $n+1$ as a relay BS, the SINR of the backhaul connection is described as:

$$SINR_{n,n+1}^{(B)} = \frac{p_{n,n+1}^{(rx)}}{B_n\sigma + \sum_{w_{n+1}} p_{w_{n+1}}^{(tx)} g_{w_{n+1},n+1}} \tag{2.11}$$

where $p_{w_{n+1}}^{(tx)}$ represents the transmission power of the interfering BS w_{n+1} from the set $\boldsymbol{N}_{n+1}^{(int)} = \{\boldsymbol{n}_1, \dots, \boldsymbol{n}_{W_{n+1}}\}$ of interference sources to the BS $n+1$ using different spectral resources than the BS n. The $g_{w_{n+1},n+1}$ then represents the propagation channel gain between the interfering BS w_{n+1} and the BS $n+1$ [15][20][21]. The SINR of the access connection between the BS $n+1$ and the UE k is then described as:

$$SINR_{n+1,k}^{(A)} = \frac{p_{n+1,k}^{(rx)}}{B_{n+1}\sigma + \sum_{w_k} p_{w_k}^{(tx)} g_{w_k,k} + p_n^{(tx)} g_{n,k}}, \tag{2.12}$$

where $p_n^{(tx)}$ represents the transmission power of the BS n using the same spectral resources as the BS $n+1$ [15][20][21]. The composition of interference in the network is demonstrated in Figure 2.3.

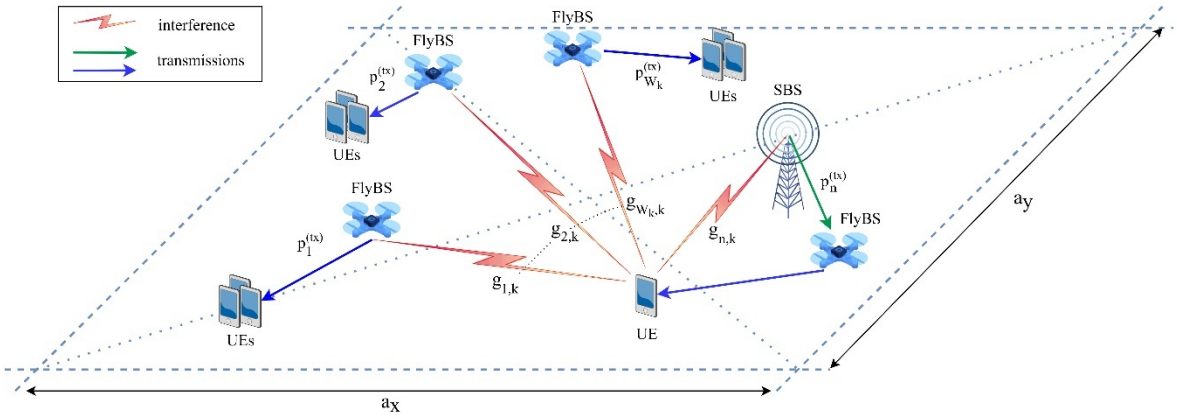

Figure 2.4 - Interference in the network

The channel capacity represents the available data rate by which the communication channel transmits data. The Shannon–Hartley theorem specifies the channel capacity, and the channel capacity of direct, backhaul, or access link according to SINR specified above is defined as [20]:

$$C_{n,k}^{(D)} = B_n * log_2\left(1 + SINR_{n,k}^{(D)}\right), \tag{2.13}$$

$$C_{n,n+1}^{(B)} = B_n * log_2\left(1 + SINR_{n,n+1}^{(B)}\right), \tag{2.14}$$

$$C_{n+1,k}^{(A)} = B_{n+1} * log_2\left(1 + SINR_{n+1,k}^{(A)}\right). \tag{2.15}$$

The channel capacity of the relay link then follows the bottleneck rule. It says the channel capacity of the relay link is defined as the minimum from the channel capacities of the backhaul and access link. Thus, the channel capacity of the relay link between the BS *n* to the UE *k,* using the BS $n + 1$ as a relay BS, is determined as [20]:

$$C_{n,k}^{(R)} = \min(C_{n,n+1}^{(B)}, C_{n+1,k}^{(A)}). \tag{2.16}$$

2.3 Caching model

Content caching represents the technique of storing popular contents in the storage of mobile network nodes, in this case, in the storage of BSs. The contents are stored both on FlyBSs and the SBS. The finite number of contents available in the network is present in the database of contents $\boldsymbol{\Psi} = \{c_1, c_2, \ldots, c_Q\}$, where Q represents the number of available contents in the network. UE requests each content with probability, which is for each UE different. It is also known as content popularity for UE. For the database $\boldsymbol{\Psi}$, the probability of content q being requested by the UE k is described by the content popularity function $\rho_k(c_q)$. The content popularity is distributed for each UE with the assumption that the sum of the popularity of all contents available in the network equals to 1 [15]. So, the distribution of content popularities for UE fulfills the prerequisite:

$$\sum_{q=1}^{Q} \rho_k(c_q) = 1\,. \tag{2.17}$$

For each content from the database $\boldsymbol{\Psi}$ is assigned the content size. For content q is the content size represented by s_q from the set of content sizes $\boldsymbol{S} = \{s_1, s_2, \ldots, s_Q\}$. The content size influences the number of contents possible to cache on BSs for limited cache storages. The content size also influences the delivery delay of the content.

Further is for contents described variable called content popularity for a group. It is defined as the probability of the content being requested by one of the UEs in the isolated group of UEs. For the BS *n* serving as a communication provider for the group of M_n UEs, the content popularity of content q for the group of M_n UEs is:

$$\rho_n(c_q) = \frac{\sum_{m_n=1}^{M_n} \rho_{m_n}(c_q)}{M_n}, \tag{2.18}$$

where the function $\rho_{m_n}(c_q)$ represents the content popularity function of the content q for m_n UE in the group served by the BS *n* [11].

The caching efficiency then evaluates the probability that one of the UEs in the BS's group requests one of the contents cached on the BS. It is calculated as the sum of content popularities of cached contents for current UEs in the group served by the BS. Thus, the caching efficiency is calculated by the formula:

$$\eta_n = \rho_n\left(c_1^{(n)}\right) + \rho_n\left(c_2^{(n)}\right) + \cdots + \rho_n\left(c_{L_n}^{(n)}\right) = \sum_{l_n=1}^{L_n} \rho_n\left(c_{l_n}^{(n)}\right), \tag{2.19}$$

where the function $P_n\left(c_{l_n}^n\right)$ represents the content popularity of the content $c_{l_n}^{(n)}$ cached on the BS *n* for the group of M_n UEs served by the BS *n* [11]. The set of contents cached in the storage of the BS *n* is represented by $\boldsymbol{\Psi_n} = \left\{c_1^{(n)}, c_2^{(n)}, \ldots, c_{L_n}^{(n)}\right\}$ where L_n is the number of contents cached in the storage of the BS *n*. To reflect (2.17), the equation (2.18) is rewritten to:

$$\eta_n = \rho_n\left(c_1^{(n)}\right) + \rho_n\left(c_2^{(n)}\right) + \cdots + \rho_n\left(c_{L_n}^{(n)}\right) = \sum_{l_n=1}^{L_n} \frac{\sum_{m_n=1}^{M_n} \rho_{m_n}\left(c_{l_n}^{(n)}\right)}{M_n}. \tag{2.20}$$

The content delivery delay we recognize the whole time between the request of the content by the UE and the moment the BS fully delivers the content to the UE [11]. The content delivery delay is dependent on the content size of the requested content, the same as on the channel capacity of the connection between the UE and the BS, which serves the UE as a communication provider. The channel capacity available for downloading the content is influenced by multiple factors and is not constant in time. For this reason, the delay calculation should consider the channel capacity's changing character. The content delivery

delay $D_{q,n,k}^{T}$ of the content q for the channel between the BS n and the UE k then comes from the relation:

$$0 = s_q - \int_{t}^{t+D_{q,n,k}^{T}} C_{n,k,t}\ dt \tag{2.21}$$

where $C_{n,k,t}$ is the capacity of a channel between the UE k and the BS n in time t.

2.4 Problem formulation

The power needed to allocate on FlyBSs for successful transmissions of content to the UEs has a significant effect on energy consumption, and the effective use of the power by FlyBSs is an essential aspect of the overall performance of the mobile network. Thus, the objective of this work is to find UE associations $\boldsymbol{A}^*$, transmission power allocation $\boldsymbol{P}^*$, and FlyBS positions $\boldsymbol{R}^*$, which minimizes the transmission power allocated by BSs for the transmission of contents and minimizes the content delivery delay. Together it reduces the energy consumed for communication in the network. The accomplishment of this goal is managed by the energy-efficient UE to BS association, transmission power navigated positioning of FlyBSs, and the deployment of more energy-efficient ways of content delivery, such as through the multi-hop relaying or FlyBS repositioning. The problem is then formulated as:

$$\boldsymbol{A}^*, \boldsymbol{P}^*, \boldsymbol{R}^{(\boldsymbol{FlyBS})^*} = \underset{\boldsymbol{A},\boldsymbol{P},\boldsymbol{R}^{(\boldsymbol{FlyBS})}}{\operatorname{argmin}} \left(\sum_{n=1}^{N} E_n \right)$$

$$\text{s.t.} \quad (2.22a) \quad P^{(tx,budget)} \geq \sum_{m_u}^{M_u} P_{u,m_u}^{(tx)} + \sum_{j}^{J} P_{u,j}^{(tx)}, \ \forall u \in \boldsymbol{U}, \tag{2.22}$$

$$(2.22b) \quad h_u \geq h_{min}, \quad \forall u \in \boldsymbol{U},$$

3 Proposed solution for formulated problem

In this Chapter are proposed mechanisms possible to implement in UAV-assisted mobile networks containing content caching to decrease the energy consumed for communication in the network. First, the UE to BS association mechanism is described, which divides UEs into groups of BSs based on providing the UEs with high channel capacity while allocating low transmission power for the content delivery on BSs. Then the algorithm of the FlyBS positioning is described, which ensures low transmission power required for the transmission of contents. Then the content popularity navigated caching scheme for BSs in the network is described. The second half of this Chapter is then devoted to the definition of how the contents are delivered to UEs, as the multi-hop relaying and FlyBS repositioning, to ensure low energy consumed for communication. The transmission power budget is defined at the end of this chapter, which limits the total transmission power allocated by FlyBSs.

3.1 UE to BS association

To ensure the low energy consumption of the network, according to (2.23), the association must take into account the transmission power needed for the transmission of the content from the particular BS, the same as the content delivery delay. It is exchanged with channel capacity as it is its main factor. Thus, to compare possible associations for UEs, the new parameter γ representing the transmission power consumption coefficient is established. The transmission power consumption coefficient for the connection between the BS n and the UE k is described as:

$$\gamma_{n,k}^{(D)} = \frac{p_{n,k}^{(tx)}}{C_{n,k}^{(D)}}. \tag{3.1}$$

The set $\boldsymbol{\gamma_k^{(UE)}} = \left\{\gamma_{1,k}^{(D)}, \dots, \gamma_{N,k}^{(D)}\right\}$ then defines the transmission power consumption coefficient for the connection to each BS in the network from the UE k. The network's energy consumption is then the smallest if every channel's transmission power consumption

coefficient is the smallest. It is managed when each UE associates with the BS, to which the transmission power consumption coefficient of the connection in $\boldsymbol{\gamma_k^{(UE)}}$ is the smallest. The problem (2.22) for UE association is then reformulated as:

$$\boldsymbol{A}^* = \underset{\boldsymbol{A}}{\operatorname{argmin}} \left(\sum_{n=1}^{n} \sum_{m_n=1}^{M_n} \gamma_{n,m_n}^{(D)} \right)$$

$$\text{s.t.} \quad (3.2a) \quad P^{(tx,budget)} \geq \sum_{m_u}^{M_u} P_{u,m_u}^{(tx)} + \sum_{j}^{J} P_{u,j}^{(tx)}, \ \forall u \in \boldsymbol{U}, \tag{3.2}$$

$$(3.2b) \quad h_u \geq h_{min}, \quad \forall u \in \boldsymbol{U},$$

where $\gamma_{n,m_n}^{(D)}$ represents the transmission power consumption coefficient of the direct connection between the BS n and the UE m_n in the group of the BS n.

The association mechanism is demonstrated by Algorithm 3.1. The first lines show the measurement and calculation of the parameters of channels between the UE and the BSs. The transmission power consumption coefficient of each of these channels is then calculated. In lines 7 to 11, it is followed by the determination of the BS with the channel of the smallest transmission power consumption coefficient and the association establishment between the UE and the BS.

Algorithm 3.1 Association of UEs to BSs

1: **for** k = 1:K
2: **for** n = 1:N
3: Measure the $SINR_{n,k}^{(D)}$ according to (2.10)
4: Calculate the channel capacity $C_{n,k}^{(D)}$ according to the $SINR_{n,k}^{(D)}$ using (2.13)
5: Calculate the power consumption coefficients $\gamma_{n,k}^{(UE)}$ in $\boldsymbol{\gamma_k^{(UE)}}$ using (3.1)
6: **end**
7: **for** n = 1:N
8: **if** min($\boldsymbol{\gamma_k^{(D)}}$) = $\gamma_{n,k}^{(D)}$ **do**
9: $a_{n,k}^{UE} = 1$, the UE k associates to the BS n
10: **end**
11: **end**
12: **end**

3.2 Positioning of FlyBSs

In the proposed system, the received power is constant, and the transmission power needed for the transmission of content through each channel from the serving FlyBS changes in time according to the movement of UEs and FlyBS itself. The energy consumed for communication of each FlyBS is composed of transmission powers allocated for transmitting contents to UEs in its group. The positioning of each FlyBS should then be set on the location, ensuring the lowest sum of transmission powers needed for transmitting contents to UEs in its group. The problem of the FlyBS positions (2.22) is then reformulated as:

$$\boldsymbol{R}^{(\boldsymbol{FlyBS})^*} = \underset{\boldsymbol{R}^{(\boldsymbol{FlyBS})}}{\operatorname{argmin}} \left(\sum_{u=1}^{U} \sum_{m_u=1}^{M_u} p_{u,m_u}^{(tx)} \right)$$

$$\text{s.t.} \quad \text{(3.3a)} \quad P^{(tx,budget)} \geq \sum_{m_u}^{M_u} P_{u,m_u}^{(tx)} + \sum_{j}^{J} P_{u,j}^{(tx)}, \ \forall u \in \boldsymbol{U}, \tag{3.3}$$

$$\text{(3.3b)} \quad h_u \geq h_{min}, \quad \forall u \in \boldsymbol{U},$$

The transmission power required for transmitting contents from the FlyBS to the UE, according to (2.7) and the definition of constant received power, is equivalent to the communication distance of transmission. It depends on the horizontal distance of the UE from the FlyBS and the operating altitude of the FlyBS, which is dependent on the horizontal distances of the UEs in its group. The positioning of FlyBSs should then search for a position ensuring the lowest sum of communication distances from UEs in its group. The problem of FlyBS positions (2.22) is then again reformulated as:

$$\boldsymbol{R}^{(\boldsymbol{FlyBS})^*} = \underset{\boldsymbol{R}^{(\boldsymbol{FlyBS})}}{\operatorname{argmin}} \left(\sum_{u=1}^{U} \sum_{m_u=1}^{M_u} d_{u,m_u} \right)$$

$$\text{s.t.} \quad \text{(3.4a)} \quad P^{(tx,budget)} \geq \sum_{m_u}^{M_u} P_{u,m_u}^{(tx)} + \sum_{j}^{J} P_{u,j}^{(tx)}, \ \forall u \in \boldsymbol{U}, \tag{3.4}$$

$$\text{(3.4b)} \quad h_u \geq h_{min}, \quad \forall u \in \boldsymbol{U},$$

The intention is to provide instant UE to BS connections of low transmission power requirement to all UEs. For this reason, the problem formulation accounts for the communication distance of all UEs in FlyBSs' groups, even UEs not requesting the content.

Suppose the problem formulation would account for the communication distance of only active UEs in FlyBSs' groups. In that case, the excessive short-term transmission power requiring channels could occur in the case of UEs outside of the FlyBSs' coverage, which would significantly affect the energy consumed for communication in the network.

Then, the x and y coordinates of the FlyBS u are defined as:

$$x_u^{(FlyBS)} = \frac{\sum_{m_u}^{M_u} x_{m_u}^{(UE)}}{M_u}, \tag{3.5}$$

$$y_u^{(FlyBS)} = \frac{\sum_{m_u}^{M_u} y_{m_u}^{(UE)}}{M_u}, \tag{3.6}$$

where $x_{m_u}^{(UE)}$ and $y_{m_u}^{(UE)}$ are x and y coordinates of UE m_u in the group of the FlyBS u. The operating altitude of the FlyBS u is then calculated according to (2.3).

The positioning of FlyBSs is demonstrated by Algorithm 3.2. First are measured the UE communication distances in FlyBS's group, as is shown in lines 2 to 4. It is followed by calculating the coordinates for FlyBSs, in lines 5 to 7.

Algorithm 3.2 Positioning of FlyBSs

1: **for** u = 1:U
2: **for** m_u = 1:M_u
3: Measure $d_{u,m_u}^{(UE)}$ in $\boldsymbol{d_u^{(UE)}}$
4: **end**
5: Calculate the x coordinate $x_u^{(FlyBS)}$ of the FlyBS u according to (3.5)
6: Calculate the y coordinate $y_u^{(FlyBS)}$ of the FlyBS u according to (3.6)
7: Calculate the operating altitude h_u of the FlyBS u according to (2.3)
8: **end**

3.3 Caching scheme

The cached contents for each BS are selected from the finite database of contents $\boldsymbol{\Psi}$ according to the content popularity for the group. The number of contents cached in the storages of BSs is influenced by the size of cache storages, the same as by the size of contents meant to be stored in these storages. The size of storage of each BS is assumed to be finite and defined by a variable in the set $\boldsymbol{S}=\left\{s_1^{(BS)}, \ldots, s_N^{(BS)}\right\}$. With the limited storage on BSs, only the contents with the highest content popularity for the group of UEs served by the BS are cached in the storage of the BS. The content popularity for the group of UEs is described in Chapter 2.3. The content q is then cached in the storage of the BS n if its content popularity for the group of UEs served by the BS n is $\rho_n(c_q) = \max\left(\boldsymbol{\rho_n^{(N)}}\right)$, where $\boldsymbol{\rho_n^{(N)}}$ is a set of content popularities for the group of UEs served by the BS n of contents not yet cached in the storage of the BS n. The set $\boldsymbol{\Psi_n} = \left\{c_1^{(n)}, \ldots, c_{L_n}^{(n)}\right\}$ then defines the contents cached in the storage of the BS n, where L_n represents the number of contents cached in the storage of the BS n, and the content sizes of cached contents are present in the set $\boldsymbol{S_n} = \left\{s_1^{(n)}, \ldots, s_{L_n}^{(n)}\right\}$. The variable $s_n^{(BS)}$ represents the limited size of cache storage on the BS n, and the remaining space in the storage $s_n^{(BS,remain)}$ is then defined as:

$$s_n^{(BS,remain)} = s_n^{(BS)} - \sum_{l_n=1}^{L_n} s_{l_n}^{(n)}, \tag{3.7}$$

Thus, the content q is cached in the storage of the BS n if $\rho_n(c_q) = \max\left(\boldsymbol{\rho_n^{(N)}}\right)$, and $s_q \leq s_n^{(BS,remain)}$. If content q does not fulfill the second criterion, it is skipped, and the following content in the content popularity line is evaluated. The process of caching runs until $\min(\boldsymbol{S}) > s_n^{(BS,remain)}$, which ensures the total capacity of cache storage is used.

The demonstration of content caching with limited storage is shown on the BS n serving as the communication provider for the group of 3 UEs. In the network are four available contents with content popularities for each UE being $\boldsymbol{\rho_1}$={0.15, 0.15, 0.3, 0.4}, $\boldsymbol{\rho_2}$={0.3, 0.25, 0.15, 0.3}, $\boldsymbol{\rho_3}$={0.4, 0.1, 0.25, 0.25}. The content popularity of contents in the group is then, according to (2.18), $\boldsymbol{\rho_n}$={0.283, 0.166, 0.233, 0.316}. When the storage size s_n^{BS} =

1 GB, and the content sizes are defined by the set $\boldsymbol{S}$ ={474 MB, 152 MB, 277 MB, 328 MB} in the same order as previous sets, contents c_1, c_2 and c_4 are cached in the storage of the BS n. The content c_3 is in the content popularity line in front of content c_2, but its size exceeds the remaining storage space $s_n^{(BS,remain)}$, thus, it is skipped.

The mechanism of content caching with limited cache storage size is demonstrated by Algorithm 3.3. In line 2 are calculated the content popularities for the group of M_n UEs served by the BS n according to (2.18). Then, in lines 3 to 17, the cached contents are determined in the cycle of conditions for each content. If the content fulfills the established criteria, present in lines 5 and 6, the number of contents on the BS increases, and the content is cached in the storage of the BS. The set $\boldsymbol{\rho_n^{(N)}}$ is then recalculated. If content does not fulfill the second criterion, the content is skipped from the caching process, as is described in line 13.

Algorithm 3.3 Caching of contents in the limited storage of BSs

1: **for** n = 1:N
2: Calculate the content popularities for the group of M_n UEs served by the BS n in $\boldsymbol{\rho_n^{(N)}}$ according to (2.18)
3: **for** q = 1:Q
4: **while** min($\boldsymbol{S}$) < $s_n^{(BS,remain)}$
5: **if** $\rho_n(c_q) = \max\left(\boldsymbol{\rho_n^{(N)}}\right)$ **do**
6: **if** $s_q \leq s_n^{(BS,remain)}$ **do**
7: $L_n = L_n + 1$, an increase in the number of contents on the BS n
8: $s_{L_n}^{(n)} = s_q$, add s_q in $\boldsymbol{S_n}$
9: $c_{L_n}^{(n)} = c_q$, add c_q in $\boldsymbol{\Psi_n}$
10: Reestablishment of $\boldsymbol{\rho_n^{(N)}}$
11: $s_n^{(BS,remain)}$ recount according to (3.7)
12: **else**
13: Skip c_q
14: **end**
15: **end**
16: **end**
17: **end**
18: **end**

3.4 Multi-hop relaying

In situations where the requested content is cached in the storage of the BS that does not offer the lowest transmission power consumption coefficient for transmitting content to the requesting UE, according to Chapter 3.1, the analysis of possible relaying is deployed. This analysis searches for the transmission paths, using other BSs as middle nodes of the connection, that would offer a lower transmission power consumption coefficient than the direct connection between UE requesting the content and BSs with cached contents. Thus, the problem (2.22) for the UE association and power allocation is reformulated as:

$$\boldsymbol{A}^*, \boldsymbol{P}^* = \underset{\boldsymbol{A},\boldsymbol{P}}{\operatorname{argmin}} \left(\sum_{n=1}^{N} \sum_{k=1}^{K} \gamma_{n,k} \right)$$

$$s.t. \quad (3.8a) \quad P^{(tx,budget)} \geq \sum_{m_u}^{M_u} P_{u,m_u}^{(tx)} + \sum_{j}^{J} P_{u,j}^{(tx)}, \ \forall u \in \boldsymbol{U}, \qquad (3.8)$$

$$(3.8b) \quad h_u \geq h_{min}, \quad \forall u \in \boldsymbol{U},$$

The proposed mechanism exploits the multi-hop relaying with channels over multiple BSs in the network. The multi-hop relay link comprises one access link between a UE and a relay BS and multiple backhaul links between relay BSs. [3] The composition of links in the multi-hop relay link is represented in Figure 3.1.

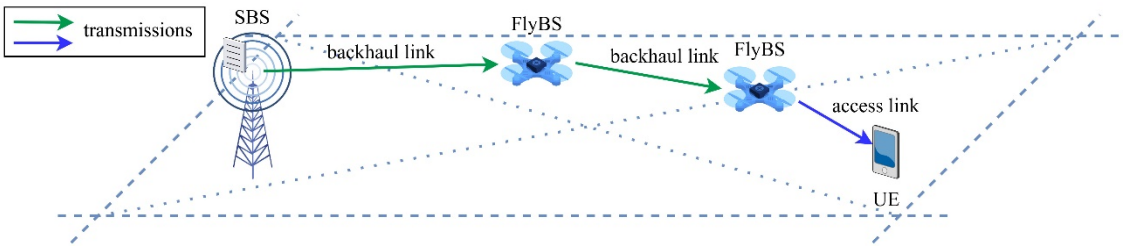

Figure 3.1 - Multi-hop relay link

In the network with multiple BSs are multiple relay transmission paths for each content delivery. The decision of the transmission path for the delivery of the content between the BS n to the UE k is made based on the transmission power consumption coefficient $\gamma_{n,k,y}^{(mR)}$ for each of Y paths. The coefficient is dependent on the multi-hop channel capacity $C_{n,k,y}^{(mR)}$,

which is significantly influenced by the interference from the backhaul. The SINR and channel capacity for multi-hop relay links are described in the following two sections. The third section then describes the transmission power $p_{n,k,y}^{(tx,mR)}$ needed for transmitting contents via multi-hop relay links, which also plays a part in assessing the coefficient value. The last section describes the decision mechanism between multi-hop relay transmission paths and the transmitting BSs.

3.4.1 Interference in multi-hop relay link

The composition of the multi-hop relay link from the access link and multiple backhaul links cause interference from the BSs using the same spectral resources. The transmission powers of the BSs participating in the multi-hop relay link interfere with the receiving UE. It is represented in Figure 3.2.

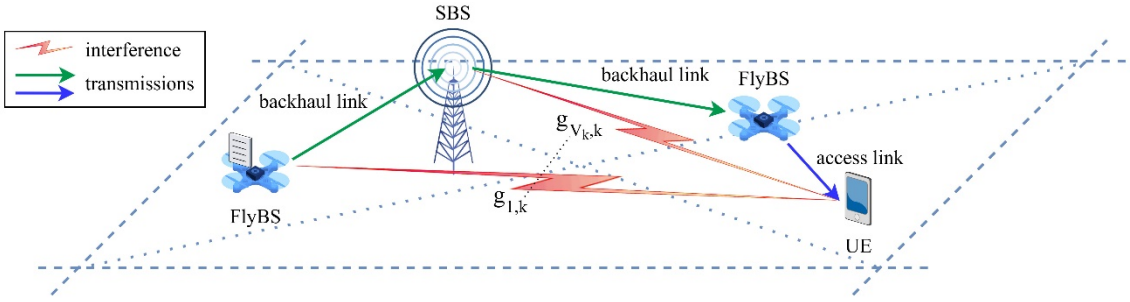

Figure 3.2 – Interference on UE in the multi-hop relay link

If the multi-hop relay link is composed of the BSs defined by the set $N_{n,k}^{(mR)} = \{n_1^{(mR)}, \dots, n_{N_{n,k}}^{(mR)}\}$, where indices of the BSs in the multi-hop relay link increase in the order of the relay link, the SINR of the access connection between the BS $N_{n,k}$, which is last in the relay link order, and the UE k is described as:

$$SINR_{N_{n,k},k}^{(A,mR)} = \frac{p_{N_{n,k},k}^{(rx)}}{B_{N_{n,k}}\sigma + \sum_{w_k} p_{w_k}^{(tx)} g_{w_k,k} + \sum_{v_k} p_{v_k}^{(tx)} g_{v_k,k}}, \tag{3.9}$$

where $p_{v_k}^{(tx)}$ represents transmission power of the interfering BS v_k from the set $\boldsymbol{N_k^{(int,R)}} = \{n_1, \dots, n_{V_k}\}$ of interference sources to the UE k using the same spectral resources as the transmitter of the transmission.

Also, the transmission powers of the BSs participating in the multi-hop relay link interfere with other BSs in the relay link. Figure 3.3 demonstrates the backhaul interference between BSs. It shows the FlyBS on the access link interferes with the SBS on the first backhaul link, and the FlyBS on the first backhaul link interferes with the FlyBS on the second backhaul link.

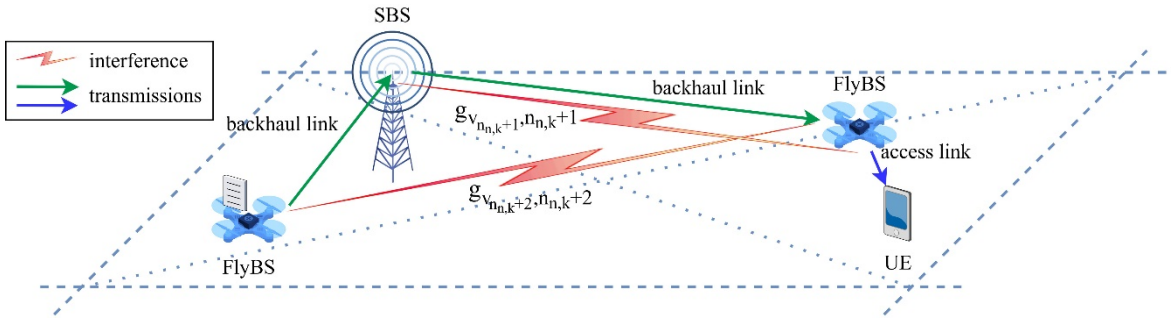

Figure 3.3 - Interference between BSs in the multi-hop relay link

The SINR of the backhaul connection between the BS $n_{n,k}$ and the BS $n_{n,k}+1$ is then described as:

$$SINR^{(B,mR)}_{n_{n,k},n_{n,k}+1} = \frac{p^{(rx)}_{n_{n,k},n_{n,k}+1}}{B_{n_{n,k}}\sigma + \sum_{w_{n_{n,k}+1}} p^{(tx)}_{w_{n_{n,k}+1}} g_{w_{n_{n,k}+1},n_{n,k}+1} + \sum_{v_{n_{n,k}+1}} p^{(tx)}_{v_{n_{n,k}+1}} g_{v_{n_{n,k}+1},n_{n,k}+1}} \quad (3.10)$$

where $p^{(tx)}_{w_{n_{n,k}+1}}$ represents the transmission power of the interfering BS $w_{n_{n,k}+1}$ from the set $\boldsymbol{N^{(int)}_{n_{n,k}+1}} = \{n_1, \dots, n_{W_{n_{n,k}+1}}\}$ of interference sources to the BS $n_{n,k}+1$ using different spectral resources than the transmitter of the transmission. The $p^{(tx)}_{v_{n_{n,k}+1}}$ then represents the transmission power of the interfering BS v_{n_k+1} from the set $\boldsymbol{N^{(int,mR)}_{n_{n,k}+1}} = \{n_1, \dots, n_{V_{n_{n,k}+1}}\}$ of interference sources to the BS $n_{n,k}+1$ using the same spectral resources as the transmitter of the transmission. The $g_{w_{n_{n,k}+1},n_{n,k}+1}$ and $g_{v_{n_{n,k}+1},n_{n,k}+1}$ represent the propagation channel gains between the interfering BSs and the BS $n_{n,k}+1$.

3.4.2 Channel capacity of multi-hop relay link

The channel capacity of access and backhaul links in the multi-hop relay is determined as:

$$C_{n_{n,k},n_{n,k}+1}^{(B,mR)} = B_{n_{n,k}} * log_2\left(1 + SINR_{n_{n,k},n_{n,k}+1}^{(B,mR)}\right), \tag{3.11}$$

$$C_{N_{n,k},k}^{(A,mR)} = B_{N_{n,k}} * log_2\left(1 + SINR_{N_{n,k},k}^{(A,mR)}\right). \tag{3.12}$$

The bottleneck rule then determines the channel capacity of the multi-hop relay link as the minimum from the channel capacities of each link in the relay link. If the BSs participating in the multi-hop relay link on transmission path y between the BS n and the UE k are defined by the set $\boldsymbol{N_{n,k,y}^{(mR)}} = \{n_1^{(mR)}, \dots, n_{N_{n,k,y}}^{(mR)}\}$, and set $\boldsymbol{C_{n,k,y}^{(mR)}} = \left\{C_{1,2}^{(B,mR)}, \dots, C_{N_{n,k,y}-1,N_{n,k,y}}^{(B,mR)}, C_{N_{n,k,y},k}^{(A,mR)}\right\}$ defines the channel capacities of connections in the relay link, then the channel capacity of the multi-hop relay link on the transmission path y is defined as:

$$C_{n,k,y}^{(mR)} = \min\left(\boldsymbol{C_{n,k,y}^{(mR)}}\right). \tag{3.13}$$

The channel capacity of the multi-hop relay link between the BS n and the UE k for each path is then in the set $\boldsymbol{C_{n,k}^{(R)}} = \left\{C_{n,k,1}^{(R)}, \dots, C_{n,k,Y}^{(R)}\right\}$.

3.4.3 Transmission power for multi-hop relay link

The transmission power needed for transmitting contents over the multi-hop relay link is determined as a sum of transmission powers needed for transmitting contents over each link in the relay link. It is for each link calculated according to (2.7). Thus, the transmission power required for the transmission of contents over the transmission path y between the BS n and the UE k, with transmission powers for each link defined by the set $\boldsymbol{P_{n,k,y}^{(mR)}} = \left\{p_{1,2}^{(tx,y)}, \dots, p_{N_{n,k,y}-1,N_{n,k,y}}^{(tx,y)}, p_{N_{n,k,y},k}^{(tx,y)}\right\}$, is determined as:

$$p_{n,k,y}^{(tx,mR)} = \sum_{n_{n,k,y}=2}^{N_{n,k,y}} p_{n_{n,k,y}-1,n_{n,k,y}}^{(tx,y)} + p_{N_{n,k,y},k}^{(tx,y)} \tag{3.14}$$

The transmission power needed for the transmission of content between the BS n and the UE k for each path is then in the set $\boldsymbol{P_{n,k}^{(mR)}} = \left\{p_{n,k,1}^{(tx,mR)}, \dots, p_{n,k,Y}^{(tx,mR)}\right\}$.

3.4.4 Path determination of multi-hop relay link

The path for the multi-hop relay link is determined based on the transmission power consumption coefficient for the transmission of contents over each path. The transmission power consumption coefficient for transmission path *y* is defined as:

$$\gamma_{n,k,y}^{(mR)} = \frac{p_{n,k,y}^{(tx,mR)}}{C_{n,k,y}^{(mR)}}. \tag{3.15}$$

The transmission power consumption coefficients for all *Y* paths between the BS *n* and the UE *k* are then defined by the set $\boldsymbol{\gamma}_{\boldsymbol{n,k}}^{(\boldsymbol{mR})} = \left\{\gamma_{n,k,1}^{(mR)}, \dots, \gamma_{n,k,Y}^{(mR)}\right\}$.

Afterward, the transmission path *y* is chosen for the transmission of contents between the BS *n* and the UE *k* if its transmission power consumption coefficient $\gamma_{n,k,y}^{(mR)}$ is the smallest from the set $\boldsymbol{\gamma}_{\boldsymbol{n,k}}^{(\boldsymbol{mR})}$. Thus, the transmission power consumption coefficient $\gamma_{n,k}^{(mR)}$ of the chosen transmission path from the transmitting BS *n* is determined as:

$$\gamma_{n,k}^{(mR)} = \min\left(\boldsymbol{\gamma}_{\boldsymbol{n,k}}^{(\boldsymbol{mR})}\right). \tag{3.16}$$

If the requested content is cached on multiple BSs, a calculation of the transmission power consumption coefficient of the chosen transmission path is made from each BS holding the content, and the coefficients are gathered in the set $\boldsymbol{\gamma}_{\boldsymbol{k}}^{(\boldsymbol{mR})} = \left\{\gamma_{1,k}^{(mR)}, \dots, \gamma_{N,k}^{(mR)}\right\}$. The transmitting BS is then determined as the BS offering the transmission path with the smallest transmission power consumption coefficient.

The process of determining the transmitting BS and transmission path for the content delivery to the UE *k* is shown in Algorithm 3.4. The first section of the algorithm from lines 2 to 15, using cycles for the BSs and transmission paths, determines the transmission power consumption coefficient for each transmission path between the UE *k* and the BSs holding the requested content. In lines 9 to 13 are then selected paths from the BSs holding the content with the smallest transmission power consumption coefficient. The second half of the algorithm in lines 16 to 27 determines the BS with the path of the smallest transmission power consumption coefficient and establishes backhaul links between the BSs in the chosen

transmission path. The association between the UE k and the last BS in the relay link order is then assembled.

Algorithm 3.4 Determination of the path of the multi-hop relay link

for k = 1:K
  for n = 1:N
    if the requested content q is cached on the BS n **do**
      for y = 1:Y
        Measure the SINR of access and backhaul links in the path y according to (3.9) and (3.10)
        Calculate the relay channel capacity $C_{n,k,y}^{(mR)}$ in $\boldsymbol{C}_{\boldsymbol{n,k}}^{(\boldsymbol{mR})}$ using (3.11), (3.12) and (3.13)
        Calculate the transmission power consumption coefficient $\gamma_{n,k,y}^{(mR)}$ in $\boldsymbol{\gamma}_{\boldsymbol{n,k}}^{(\boldsymbol{mR})}$ using (3.15)
      end
      for y = 1:Y
        if $\min(\boldsymbol{\gamma}_{\boldsymbol{n,k}}^{(\boldsymbol{mR})}) = \gamma_{n,k,y}^{(mR)}$ && $\gamma_{n,k,y}^{(mR)} < \gamma_{n,k}^{(D)}$ **do**
          $\gamma_{n,k}^{(mR)} = \gamma_{n,k,y}^{(mR)}$
          Add $\gamma_{n,k}^{(mR)}$ in $\boldsymbol{\gamma}_{\boldsymbol{k}}^{(\boldsymbol{mR})}$
        end
      end
    end
  end
  for n = 1:N
    if $\min(\boldsymbol{\gamma}_{\boldsymbol{k}}^{(\boldsymbol{mR})}) = \gamma_{n,k}^{(mR)}$
      for y = 1:Y
        if $\gamma_{n,k}^{(mR)} = \gamma_{n,k,y}^{(mR)}$
          $a_{N_{n,k,y},k}^{UE} = 1$, the UE k associates to the last BS in the path y
          for $n_{n,k,y}$ = 2:$N_{n,k,y}$
            $a_{n_{n,k,y}-1,n_{n,k,y}}^{BS} = 1$, the backhaul link established between the BSs in the path y
          end
        end
      end
    end
  end
end

3.5 Repositioning of FlyBSs

Another improvement of the mobile network containing FlyBSs and relaying is making the FlyBSs move toward the UEs requesting the content if it is beneficial from the energy consumption perspective. The evaluation of this mechanism deploys when the relay link is found as the best option for transmitting content from the FlyBS to the UE. This mechanism searches for the position of the transmitting FlyBS, which would make transmitting the requested content by the direct link less power-demanding than transmitting by the relay link. At the same time, this mechanism searches for the position of the FlyBS, resulting in lower energy consumed for communication by the FlyBS than in the original position. So, this mechanism influences the UE association, power allocation, and FlyBS position. The problem (2.22) is then reformulated, similarly as for the multi-hop relaying, as:

$$\boldsymbol{A}^*, \boldsymbol{P}^*, \boldsymbol{R}^{(\boldsymbol{FlyBS})^*} = \underset{\boldsymbol{A},\boldsymbol{P},\boldsymbol{R}^{(\boldsymbol{FlyBS})}}{\operatorname{argmin}} \left(\sum_{n=1}^{N} \sum_{k=1}^{K} \gamma_{n,k} \right)$$

$$s.t. \quad (3.17a) \quad P^{(tx,budget)} \geq \sum_{m_u}^{M_u} P_{u,m_u}^{(tx)} + \sum_{j}^{J} P_{u,j}^{(tx)}, \ \forall u \in \boldsymbol{U}, \tag{3.17}$$

$$(3.17b) \quad h_u \geq h_{min}, \quad \forall u \in \boldsymbol{U},$$

The illustration of the mechanism is demonstrated in Figure 3.4.

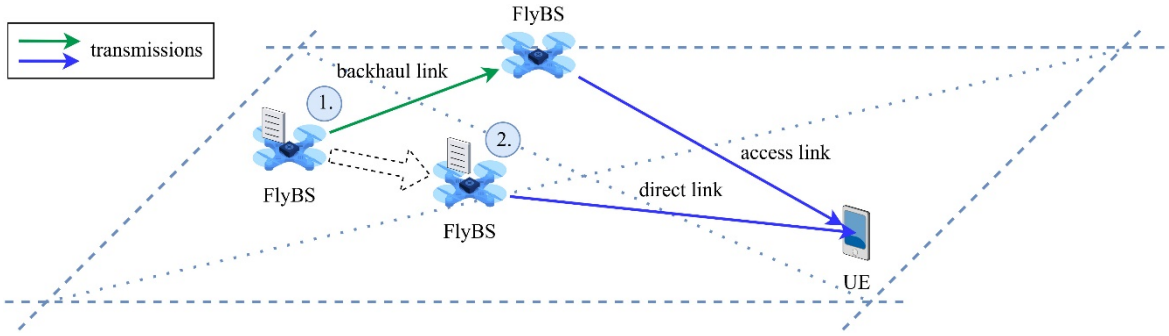

Figure 3.4 - Reposition of FlyBS

The evaluation of this mechanism is based on set criteria, described in the following section, and on the repositioning coordinates determination, described in the last section of this Chapter.

3.5.1 Repositioning criteria

The first criterion, to allow the reposition of the FlyBS *u,* says the transmission power consumption coefficient $\gamma_{u,k}^{(poz2)}$ of the direct link between the FlyBS *u* and the UE *k* from the new position of the FlyBS *u* must be smaller than the transmission power consumption coefficient $\gamma_{u,k}^{(poz1)}$ of the relay link between the FlyBS *u* and the UE *k* from the original position. The first criterion is then described as:

$$\gamma_{u,k}^{(poz1)} \geq \gamma_{u,k}^{(poz2)}, \tag{3.18}$$

where $\gamma_{u,k}^{(poz1)}$ is equal to the transmission power consumption coefficient $\gamma_{n,k}^{(R)}$ of the chosen relay link path between the FlyBS *u* and the UE *k*.

The second criterion is then assembled to ensure the reposition of the FlyBS *u* doesn't negatively affect the energy consumed for communication by the FlyBS *u*. This criterion says the sum of the transmission power consumption coefficients of channels from the FlyBS *u* to the UEs in its group from the new position must be smaller than from the original position. The second criterion is then described as:

$$\sum_{m_u=1}^{M_u} \gamma_{u,m_u}^{(poz1)} \geq \sum_{m_u=1}^{M_u} \gamma_{u,m_u}^{(poz2)}. \tag{3.19}$$

3.5.2 Repositioning coordinates

The repositioning coordinates are determined according to the criteria described in the previous section. The coordinates determination is based on the assumption that the direct link channel capacity from the FlyBS *u* to the UE k does not change significantly after repositioning. This assumption is based on the guarantee of the received power $p_{u,k}^{(tx)}$, thus the $SINR_{u,k}^{(D)}$ should not change. By this assumption, the maximal communication distance between the FlyBS *u* and the UE *k* to fulfill the first criterion is possible to calculate from the following relation, which represents the first criterion in a different form:

$$\frac{p_{u,k}^{(tx,R,poz1)}}{C_{u,k}^{(R)}} \geq \frac{p_{u,k}^{(tx,poz2)}}{C_{u,k}^{(D)}}. \tag{3.20}$$

In the relation (3.20), the only unknown variable is $p_{u,k}^{(tx,poz2)}$, which represents the transmission power needed for transmitting contents between the FlyBS u to the UE k from its new position. As all other variables are known, $p_{u,k}^{(tx,poz2)}$ can be calculated. According to (2.7) and (2.5) is then calculated the maximal communication distance $D_{u,k}^{(\max)}$ of the direct link between the FlyBS u to the UE k, which fulfills the first criterion.

The position for the repositioning of FlyBS is then searched on the curve of the maximal communication distance $D_{u,k}^{(\max)}$. The possible positions for the repositioning of FlyBS are demonstrated in Figure 3.5.

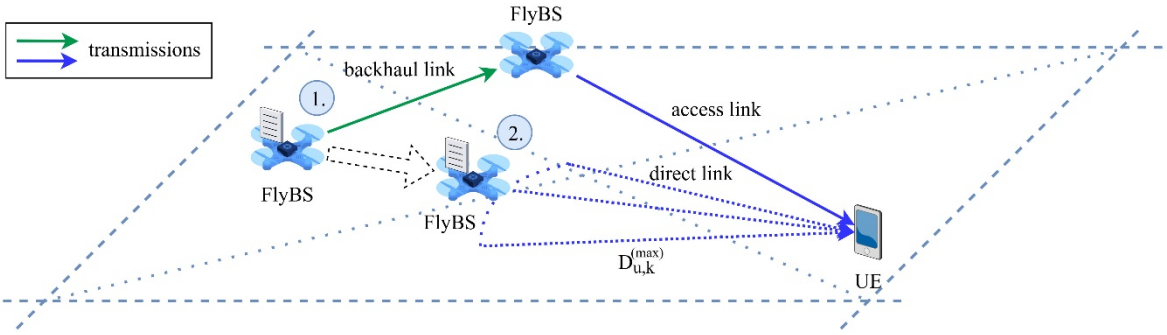

Figure 3.5 - Reposition coordinates of FlyBS

The sum of the transmission power consumption coefficients of channels from the FlyBS u to UEs in its group is calculated for Z positions on the curve of $D_{u,k}^{(\max)}$ with a spacing angle equal to φ. The operation altitude of the FlyBS u for each position on the curve of $D_{u,k}^{(\max)}$ follows (2.3). The sum of transmission power consumption coefficients of UE-directed channels from the FlyBS u in the position z is described as:

$$\gamma_{u,z}^{(BS)} = \sum_{m_u=1}^{M_u} \gamma_{u,m_u}^{(pos\ z)} \tag{3.21}$$

where $\gamma_{u,m_u}^{(pos\ z)}$ represents the transmission power consumption coefficient of the channel between the FlyBS u and the UE m_u from the position z. The set $\boldsymbol{\gamma_u^{(BS,poz2)}} =$

$\left\{\gamma_{u,1}^{(BS)}, \ldots, \gamma_{u,Z}^{(BS)}\right\}$ then contains sums of transmission power consumption coefficients of channels from the FlyBS u in Z positions. Afterward, the position z is determined as the most promising position if $\gamma_{u,z}^{(BS)}$ equals to the minimum of $\boldsymbol{\gamma_u^{(BS,poz2)}}$. Hence, the second criterion for the repositioning of the FlyBS u is fulfilled if:

$$\sum_{m_u=1}^{M_u} \gamma_{u,m_u}^{(poz1)} \geq \min\left(\boldsymbol{\gamma_u^{(BS,poz2)}}\right) \tag{3.22}$$

applies. If the first and second criteria are fulfilled, the reposition of the FlyBS u is assembled.

The whole process of the repositioning of FlyBS is described by Algorithm 3.6. The first two lines of the algorithm confirm the content q requested by the UE k is cached on the FlyBS u. The following line 3 confirms the most beneficial transmission path from the energy efficiency perspective is the one via relay link. The parameters needed for evaluating the fulfillment of repositioning criteria for Z positions of the FlyBS u are then calculated in lines 4 to 7. The cycle of conditions in lines 8 to 10 determines the most promising repositioning position of the FlyBS u. In case the sum of transmission power consumption coefficients of channels from the FlyBS u in the new position fulfills the second criterion for repositioning, the FlyBS u repositions to the new position, as described in lines 11 to 15.

Algorithm 3.6 Repositioning of FlyBSs

1: **for** $u = 1{:}U$
2: **if** requested content q is cached on the FlyBS u **do**
3: **if** $\min(\boldsymbol{\gamma_{u,k}^{(R)}}) < \gamma_{u,k}^{(D)}$ **do**
4: Calculate $D_{u,k}^{(\max)}$ using (3.20), (2.7) and (2.5)
5: **for** $z = 1{:}Z$
6: Calculate $\gamma_{u,z}^{(BS)}$ in $\boldsymbol{\gamma_u^{(poz2)}}$ using (3.21)
7: **end**
8: **for** $z = 1{:}Z$
9: **if** $\gamma_{u,z}^{(BS)} = \min\left(\boldsymbol{\gamma_u^{(BS,poz2)}}\right)$ **do**
10: **if** $\gamma_{u,k}^{(poz1)} \geq \gamma_{u,k}^{(poz2)}$ && $\sum_{m_u=1}^{M_u} \gamma_{u,m_u}^{(poz1)} \geq \gamma_{u,z}^{(BS)}$ **do**
11: $a_{n,k}^{(UE)} = 1$, the UE k associates to the BS n
12: $x_u^{(FlyBS)} = x_{u,z}^{(FlyBS)}$, $y_u^{(FlyBS)} = y_{u,z}^{(FlyBS)}$
13: $\boldsymbol{d_u^{(UE)}}$ is updated according to the new coordinates of the FlyBS u

```
14:                     h_u operation altitude is calculated according to (2.3)
15:                 end
16:             end
17:         end
18:     end
19: end
20: end
```

3.6 Transmission power budget

For each FlyBS is set the transmission power budget $P^{(tx,budget)}$ representing the maximum sum of transmission powers the FlyBS is allowed to allocate for transmissions of contents each second. This limitation should prevent the FlyBSs from excessive power consumption, which would negatively influence the network's overall performance [17]. The sum of transmission powers allocated by the FlyBS u for transmissions of contents is required to fulfill the prerequisite:

$$P^{(tx,budget)} \geq \sum_{m_u}^{M_u} P_{u,m_u}^{(tx)} + \sum_{j}^{J} P_{u,j}^{(tx)} \ . \tag{3.23}$$

If the sum of transmission powers allocated by the FlyBS u crosses its power budget $P^{(tx,budget)}$, the FlyBS cancels the connection originating from the UE, which has the best possibility to receive the content by a different transmission path, not influencing the sum of transmission powers of the FlyBS u. In other words, disconnected is the UE, for which the smallest transmission power consumption coefficient of any different way of content delivery is the smallest from UEs influencing the sum of transmission powers of the FlyBS u. The other ways of content delivery include the content transmission from the different BS, or, in the case of relaying over the FlyBS u, the relaying is rerouted to a different transmission path, not influencing the sum of transmission powers of the FlyBS u.

The power budget control is demonstrated by Algorithm 3.7. The first section, in lines 3 to 9, after the breach of the power budget in line 2, calculates the transmission power consumption coefficients of channels from neighboring BSs to UEs in FlyBS's group. The second section in lines 10 to 18 then calculates the transmission power consumption coefficients of different paths for relay links using FlyBS as relay BS. The third section in

lines 19 to 31 determines the UE with the best possibility to receive the content without the power transmitted by the FlyBS. This UE is then disconnected or rerouted to another transmission path.

Algorithm 3.7 Transmission power budget

```
1:  for u = 1:U
2:      if the sum of transmission powers of the FlyBS u is bigger than P^(tx,budget) do
3:          for m_u = 1:M_u
4:              if UE m_u requests content do
5:                  for j_u = 1:J_u
6:                      Calculate γ^(D)_(j_u,m_u) in γ^(D)_(m_u) using (3.1)
7:                  end
8:              end
9:          end
10:         for k = 1:K
11:             for n = 1:N
12:                 if the channel from the BS n to the UE k is relaying over the FlyBS u do
13:                     for y from 1 to Y paths
14:                         Calculate γ^(R)_(n,k,y) in γ^(R)_(n,k) using (3.16)
15:                     end
16:                 end
17:             end
18:         end
19:         if min(γ^(UE)_(m_u)) < min(γ^(relay)_(n,k)) do
20:             for j_u = 1:J_u
21:                 if min(γ^(UE)_(m_u)) = γ^(UE)_(j_u,m_u) do
22:                     Reconnect the UE m_u to the BS j_u
23:                 end
24:             end
25:         else do
26:             for y = 1:Y
27:                 if min(γ^(R)_(n,k)) = γ^(UE)_(n,k,y) do
28:                     Reroute the relay link between the BS n and the UE k to the path y
29:                 end
30:             end
31:         end
32:     end
33: end
```

3.7 Content delivery possibilities

This section summarizes the possible ways the contents can be delivered to the UEs in the wireless communication network with implemented mechanisms mentioned in this Chapter. In such a network, depending on the distribution of content, three possible ways of contents delivery are evaluated:

1. **The requested content is cached on the BS with a channel of the lowest transmission power consumption coefficient**

   Suppose the requested content q of the UE k is cached in the storage of the BS n with a channel of the lowest power consumption coefficient, according to Chapter 3.1, then the transmission via direct link is established between the UE k and the BS n

2. **The requested content is not cached on the BS with a channel of the lowest transmission power consumption coefficient but is cached on another BS in the network**

   Suppose the requested content q of the UE k is not cached in the storage of the BS n with a channel of the lowest power consumption coefficient, according to Chapter 3.1, but is cached in the storage of one or multiple other BSs in the network. In that case, the relaying is evaluated, according to Chapter 3.5. In case relaying is the preferred way of content delivery, according to Chapter 3.5, and the chosen transmitting BS j_n is FlyBS, the repositioning is evaluated according to Chapter 3.6. The transmission via direct link or relay link is then established between the UE k and the BS j_n.

3. **The requested content is not cached in the network**

   Suppose the requested content q of the UE k is not cached in the storage of any BS in the network. In that case, the content q is downloaded from the core network to the SBS, and the relaying, according to Chapter 3.5, is then evaluated for the connection between the UE k and the SBS. As the SBS does not hold the ability to move, the repositioning is not evaluated. The transmission via direct link or relay link is then established between the UE k and the SBS.

4 System performance

This Chapter first covers information about the network characteristics as it is simulated, its description, behavior, and application of the proposed techniques. In the second half of this Chapter are presented the simulation results of simulation parameters for multiple network settings in comparison with related works examining the UAV-assisted mobile networks containing content caching. The related works differ in the way the contents are delivered to UEs. The simulation parameters are the energy consumed for communication in the network and the content delivery delay.

4.1 Simulation model description

The simulation simulates a restricted area sized 100 m x 100 m with one ground SBS and multiple UAVs serving as FlyBSs for the period of T = 500 s. The number of FlyBSs in the network changes during the simulation from 3 to 6. If the number is not specified differently, the number of FlyBSs in the network is 4. At the beginning of the simulation, the SBS is placed in the center of the restricted area, and FlyBSs are placed in the surrounding space to ensure each BS covers equally sized space. The positions of the FlyBSs are determined based on the size of the area and according to the calculation of FlyBSs' covered area characterized in Chapter 2.1.

In the area are randomly allocated UEs moving each second in randomized directions by the randomized speed with the maximum speed V_{max} = 2 m/s. Suppose any UE happens to reach the border of the simulation area, its direction changes by 180° to keep the UE in the area. With this strategy, the number of UEs in the simulation area stays the same for the whole simulation [11][15]. The UEs are moving on the flat surface, so there is no change in the altitude position of UEs. The number of UEs in the network changes during the simulation from 10 to 40. If the number is not specified differently, the number of UEs in the network is 30.

FlyBSs move with the maximum speed $V_{max}^{(BS)}$ = 5 m/s each second in horizontal directions (x, y coordinates) above the UEs, and with the maximum speed $V_{max}^{(BS,h)}$ = 2 m/s in altitude h. The location of FlyBS each second is determined by the movement of UEs in the groups served by FlyBS. This algorithm is described in Chapter 3.2. The operating altitude is limited, as described in Chapter 2.1, by minimal altitude h_{min} = 5 m. The simulation area does not contain any obstacles, and only line-of-sight communication is applied. The estimated average temperature of the environment in the simulation area is $T^{(envir)}$ = 283,15 K. Thus, the noise spectral density is evaluated as $\sigma = 4T^{(envir)}K = 1.56*10^{-20}$ W/Hz (−168 dBm/Hz), where K is the Boltzmann constant [3]. The simulation network example from the computing environment MATLAB is presented in Figure 4.1.

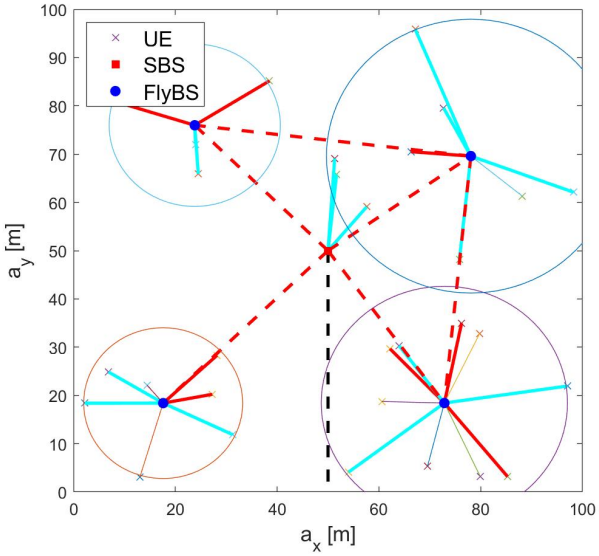

Figure 4.1 - The simulated network

The antenna used by the SBS is an omnidirectional antenna with antenna gain G_{SBS} = 10 dBi. Each FlyBS uses a semi-directional antenna with antenna gain G_{FlyBS} = 5 dBi. The angle of half of the FlyBS antenna's coverage is set at $\alpha = 60°$. The angle of the FlyBS antenna's coverage influences the operating altitude of FlyBSs, according to (2.3).

The carrier frequency band shared by all BSs is set at f = 3.4 GHz. The shared bandwidth allocated for each BS is then B = 20 MHz. The bandwidth distribution between BSs' channels in the environment with OFDMA is described in Chapter 2.2.4. The guaranteed receive power for each channel in the network is set on $p^{(rx)}$ = 0.1 μW (-40 dBm). The transmission power for each channel to deliver the content with guaranteed receive power is

then calculated according to (2.7). The FlyBS transmission power budget is then set on a value $P^{(tx,budget)}$ = 3 W (34.77 dBm). The power budget control is handled according to Chapter 3.6.

In the network are available 20 contents, where each content is assigned the content popularity for each EU described in Chapter 2.3. The content popularity for each EU is designed according to the Zipf distribution. Each content is also assigned the content size described in Chapter 2.3, designed by the Zipf distribution and influenced by the contents' content popularity for all UEs in the network. The content popularity increases the probability the content with high content popularity is assigned a smaller content size. The content size is restricted to the size span of 100 to 1000 Mbit. The cache storage size on FlyBSs changes during the simulation from 1 to 4 Gbit. If the size is not specified differently, the cache storage size on FlyBSs is 3 Gbit. The cache storage size on the SBS is then set to 3 Gbit. The content delivery delay is calculated according to (2.21). If the content is not cached in the cache storage of any BS in the network, the content delivery delay is increased by the constant variable $D^{T(core)}$ = 0.2 s for each second of download, which represents the delay caused by downloading the content from the core network. In the case of relaying, no delay caused by the hoping is considered.

The summary of the network characteristics is presented in Table 4.1.

Table 4.1 - Network characteristics

Characteristic	*Value*
Size of the simulation area	100 m x 100 m
Number of SBSs in the area	1
Number of FlyBSs in the area	3 - 6
Number of UEs in the area	10 - 40
The altitude of the SBS antenna	20 m
The altitude of the FlyBS antenna	Change in time
UE's maximum speed	2 m/s
FlyBS's maximum horizontal speed	5 m/s
FlyBS's maximum vertical speed	2 m/s

FlyBS's maximum operating altitude	30 m
FlyBS's minimum operating altitude	5 m
Noise spectral density	$1.56*10^{-20}$ W/Hz (−168 dBm/Hz)
Carrier frequency	3.4 GHz
Frequency bandwidth	20 MHz
SBS antenna gain	10 dBi
FlyBS antenna gain	5 dBi
The angle of half of the FlyBS antenna's coverage	60°
Spacing angle	4°
Guaranteed received power	0.1 μW (-40 dBm)
Transmission power budget	3 W (34.77 dBm)
SBS storage	3 Gbit
FlyBS storage	1 - 4 Gbit
Content size	100 - 1000 Mbit – Zipf distribution
Core network delay	0.2 s

4.2 Simulation results

This section presents the results of the simulated parameters for the mobile network with implemented proposed mechanisms. The results are compared to the simulated parameters for network architectures put forward in related works differing in how the contents are delivered to UEs. The comparison cannot reflect all mechanisms proposed in this thesis, thus, the comparison focuses on the content delivery scheme in these networks.

The first related work compared with the proposed network is the paper [15]. This work presents a mobile network with content caching which does not contain relaying, and the backhaul links from the SBS to the FlyBSs are established only for the purpose of caching contents. In case any UE requests content, which is not cached on any BS in the network,

the UE assembles the connection with the SBS, and the content is then delivered from the core network.

The second related work designing network compared with the proposed network is the paper [22]. The network, according to this work, contains content caching and does contain relaying in its content delivery scheme. The difference is the network suggested in [22] deploys only the single-hop relaying that is possible strictly from the SBS to the UEs. Thus, the multi-hop relaying, which may originate from the FlyBS, is not supported.

The mentioned networks are simulated for multiple network settings for 30 scenarios of UE behavior, content popularity distribution, and content size distribution. The simulation parameters results are then collected as an average from all 30 simulations and represented by the figures in the following chapters.

4.2.1 Energy consumed for communication

The first presented simulation results concern the energy consumed for communication in the network. It is simulated for multiple settings of the number of the FlyBSs in the network, the number of the UEs in the network, and the size of storage on the FlyBSs in the network.

The comparison of the proposed network with networks suggested in related works is presented in Figures 4.2 to 4.4. The change in the characteristics of the network is visible on the x-axis of the Figures. The y-axis of the Figures then represents the simulation parameter values for the according set of network characteristics. The energy consumed for the communication is first evaluated for the whole network as one entity, which is represented by Figures 4.2a, 4.3a, and 4.4a, and then separately for the SBS and the FlyBSs, which is represented by Figures 4.2b, 4.2c, 4.3b, 4.3c, 4.4b, and 4.4c.

Figure 4.2 represents the difference in energy consumed for communication between the compared networks depending on the number of the FlyBSs in the network. Figure 4.2a shows the energy consumed for communication decreases with the number of the FlyBSs in the network in the case of all compared networks. That is an outcome of a better distribution of UEs between the FlyBSs, which brings the possibility of positioning the FlyBSs closer to the UEs and decreases the communication distance of channels. Figure 4.2a shows that the energy consumed for communication in the proposed network is much lower for each

number of the FlyBSs in the network than in the networks suggested in [15] and [22]. The difference between the proposed network and the network suggested in [15] is approximately 37 % for 3 FlyBSs in the network. With the rise of the number of the FlyBSs in the network to 6, the difference increases to 54%. The difference in the energy consumed for communication in the network suggested in [22] compared to the network proposed in this thesis is approximately 39 % for 6 FlyBSs in the network. This result shows that the multi-backhaul relaying, capable of originating from FlyBS, significantly decreases the energy consumed for communication in the networks, and the decrease becomes more prominent with the rising number of the FlyBSs in the network. Figure 4.2b displays the energy consumed for communication by the SBS. It reveals that the energy consumed in the proposed network and the network put forward in [22] do not differ substantially. It is an expected outcome as the SBS in both networks has a similar role. The energy consumed for the communication by the SBS in the network put forward in [15] then notably differs as it is approximately two times higher for 6 FlyBSs than in the other two compared networks. It is based on the content delivery scheme of [15], where the SBS must transmit contents even to far-located UEs, which require high transmission power allocation. It shows the importance of relaying in mobile networks. Figure 4.2c represents the energy consumed for communication by the FlyBSs. It shows that the energy consumed for the communication by the FlyBSs in the proposed network is approximately 47% lower than in both compared networks for 6 FlyBSs. The equivalent difference can then be seen in energy consumed for communication by the FlyBSs in the proposed network and the network suggested in [22] for all numbers of the FlyBSs in the network. The difference in energy consumed for communication by the FlyBSs with the network suggested in [15] then drops to 40 % for 3 FlyBSs in the network. The difference is mainly caused by the possibility of transmitting contents from the FlyBSs through multi-hop relay links, which enables delivery to the distant UEs requiring much lower transmission power allocation. It is also important to point out in the Figure the inconsistent progression of the energy consumed for communication by the FlyBSs in the proposed network between 3 and 4 FlyBSs in the network. The progression in this section of the Figure does not exhibit a decrease in the energy consumed but constantly progresses or even exhibits a slight increase. This inconsistent progression results from the high number of UEs spread in a wide area served by the small number of the FlyBSs. The small number of the FlyBSs in the network results in significantly sized areas not covered by the FlyBSs, as the FlyBSs can provide service only to a limited number of UEs with

established power budget and limited covered area. The communication load to the UEs in areas not covered by the FlyBSs is then left on the SBS. The extra FlyBSs then supports the fill of areas not covered by the FlyBSs and take over some communication load left on the SBS. It adds significant energy to the energy consumed for communication by the FlyBSs in the network. Thus, the increase in the number of the FlyBSs by one helps with the distribution of the communication load between the BSs in the network. However, this change does not significantly influence the operation of the FlyBSs enough to overcome the extra power resulting from the communication load taken from the SBS. For this reason, the progression slightly increases. The consequent increase in the number of the FlyBSs in the network then perceptibly decreases the energy consumed for communication by the FlyBSs in the proposed network.

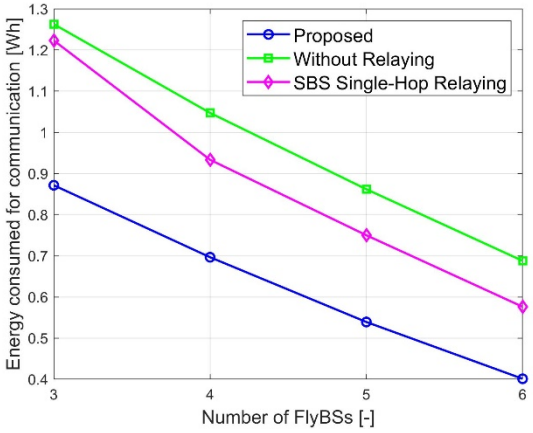

(a) for whole network

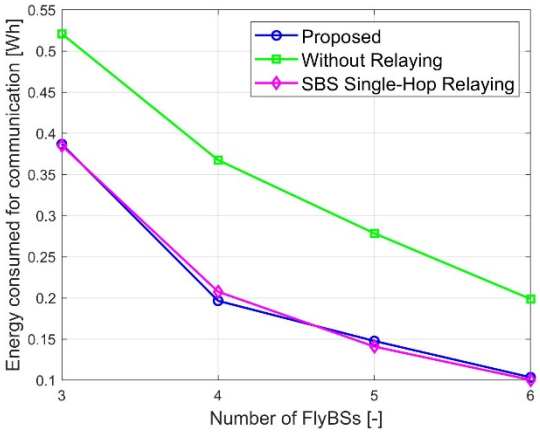

(b) for SBS

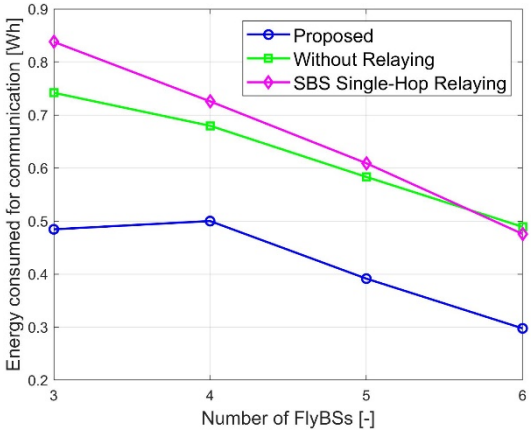

(c) for FlyBSs

Figure 4.2 - Energy consumed for communication depending on the number of FlyBSs in the network, Number of UEs K = 50, FlyBS's cache storage $s^{(BS)}$ = 3 Gbit

Figure 4.3 represents the difference in energy consumed for communication between the compared networks depending on the number of the UEs in the network. From Figure 4.3, it is possible to read out that the energy consumed for communication generally increases with the number of the UEs in the network. That is the expected outcome as the rising number of the UEs increases the number of transmissions of contents in the network requiring allocation of transmission power. Figure 4.3a shows the energy consumed for communication depending on the number of the UEs is lower in the proposed network than in the networks put forward in related works. It is possible to read out that the difference increases with the rising number of the UEs in the network, but the percentual difference decreases. In the case of 20 UEs in the network, the energy consumed for communication in the proposed network is 57% lower than in the network suggested in [22] and 66% lower than in the network suggested in [15]. In the case of 40 UEs in the network, the difference in energy consumed for communication drops to 24% compared to the network suggested in [22] and 30% compared to the network suggested in [15]. The decrease in the percentual difference between the networks depending on the number of the UEs is caused by the rise in communication demand which is not balanced by the increase in communication resources. Figure 4.3b shows that the energy consumed for communication by the SBS in the proposed network does not differ significantly from the energy consumed in the network suggested in [22]. The similar role of the SBS in both networks is again the cause of this outcome. The energy consumed for the communication by the SBS in the network suggested in [15] is then almost two times higher than in the other two compared networks. The equivalent difference can then be seen for all numbers of the UEs in the network. It demonstrates the excessive load of communication left on the SBS in the network without relaying. Figure 4.3c then displays that the energy consumed for communication by the FlyBSs in the networks suggested in related works, containing 20 UEs, is approximately 73% higher than in the network proposed in this thesis, with the same number of the UEs. This difference again decreases with the rise in the number of the UEs in the network as for 6 UEs the difference drops to 17% for [15] and 29% for [22].

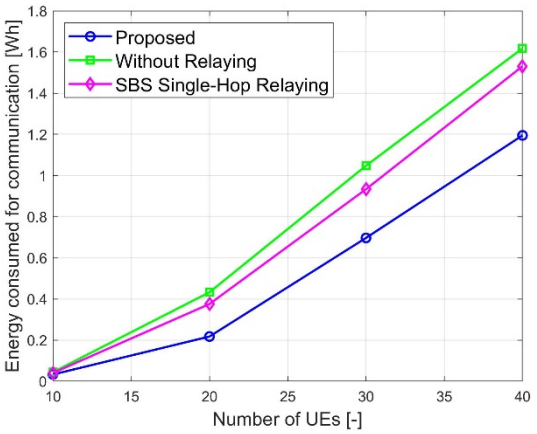

(a) for whole network

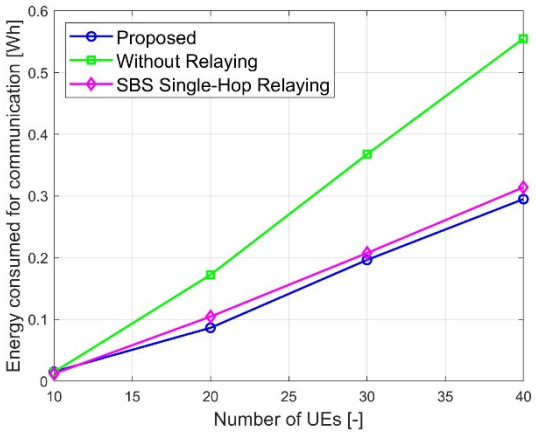

(b) for SBS

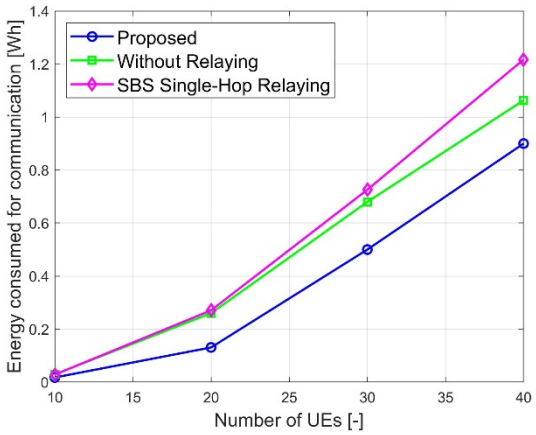

(c) for FlyBSs

Figure 4.3 - Energy consumed for communication depending on the number of UEs in the network, Number of FlyBSs U = 4, FlyBS's cache storage $s^{(BS)}$= 3 Gbit

Figure 4.4 represents the difference in the energy consumed for communication between the compared networks depending on the storage size for caching of contents on the FlyBSs in the network. It displays the decrease in energy consumed for communication with the rising size of cache storage on the FlyBSs in the case of all compared networks. The decrease is caused by the escalated availability of cached contents in the network, which increases the probability of requested contents being cached on the the FlyBSs near the UEs. Figure 4.4a demonstrates that the energy consumed for communication in the proposed network is again lower than in compared networks. The progression of energy consumed for communication in the network suggested in [22] exhibits an increase compared to the energy consumed in the proposed network by approximately 27% for all sizes of cache storage. The energy consumed for communication in the network presented in [15] is then higher by

approximately 52% in the case of 1 Gbit of cache storage size, which decreases to a difference of 37 % for 4 Gbit of cache storage size. This trend is also visible in Figure 4.4b, which shows the energy consumed for communication by the SBS. It shows that the energy consumed for communication by the SBS in the network presented in [15] is more than three times higher than in the case of the proposed network for FlyBSs' cache storage size of 1 Gbit. This difference significantly decreases with the rise of cache storage size, as the difference drops to approximately 40% for 4 Gbit of cache storage size on the FlyBSs. The substantial difference in the case of 1 Gbit cache storage size is caused by the network's low availability of cached contents, which causes small involvement of the FlyBSs in the network's communication. It subsequently forces the SBS in the network proposed in [15] to establish long-distance channels to deliver contents to the UEs. Figure 4.4c then displays the energy consumed for communication by the FlyBSs depending on their size of cache storage for each of the compared networks. The critical section to point out in this Figure is the transition of progression of energy consumed for communication by the FlyBSs in the networks suggested in [22], and especially [15], between 1 Gbit and 2 Gbit of cache storage size. The progression of the energy spent in this section increases on both networks due to the increased availability of cached contents on the FlyBSs, which induce higher involvement of the FlyBSs in the network's communication. As visible in comparison with Figure 4.4b, the comparable amount of energy consumed decreases on the SBS with the increase of cache storage size from 1 Gbit to 2 Gbit. The energy consumed for communication by the FlyBSs then decreases with a further rise of the cache storage size in these networks. This positive change results from further escalation of cached contents availability in the network, potentially enabling the FlyBSs to deliver contents to the close-situated UEs. The energy consumed for communication by the FlyBSs in the proposed network then slightly decreases with each increase in cache storage size. Importantly, the energy consumed for communication by the FlyBSs in the proposed network is lower for each size of cache storage than in compared networks suggested in the related works. The difference is approximately 36% for the cache storage size of 4 Gbit.

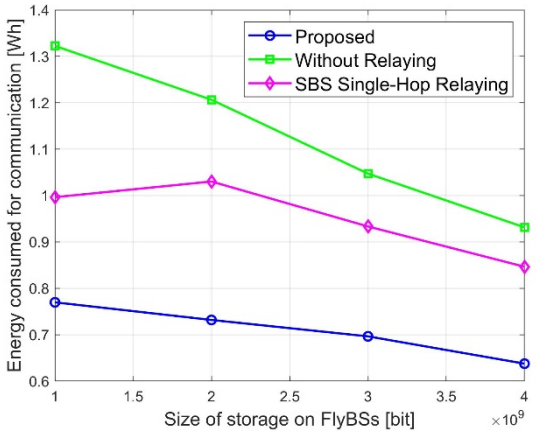

(a) for whole network

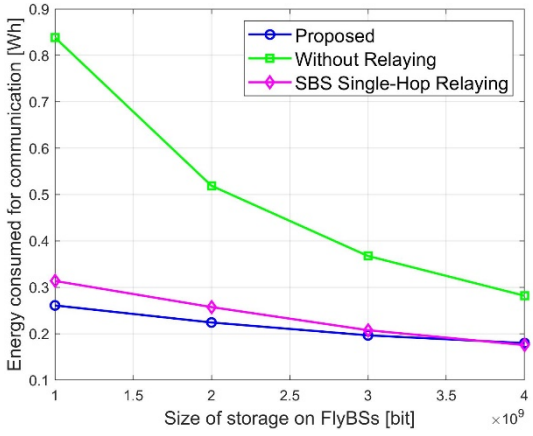

(b) for SBS

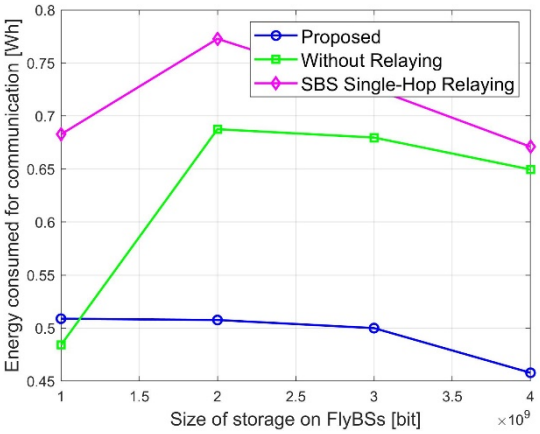

(c) for FlyBSs

Figure 4.4 - Energy consumed for communication depending on the size of cache storage on FlyBSs, Number of FlyBSs U = 4, Number of UEs K = 30

Figures 4.2 to 4.4 show that the energy consumed for communication in the proposed network with implemented proposed mechanisms is substantially lower than in the networks suggested in the related works for each set of network characteristics. It proves that the multi-hop relaying and FlyBS repositioning proposed in this thesis are essential mechanisms for the low energy consumed for communication in UAV-assisted networks containing content caching.

4.2.2 Average content delivery delay

The second presented simulation results are for average content delivery delay, equivalently simulated for multiple settings of the number of the FlyBSs in the network, the number of the UEs in the network, and the size of storage on the FlyBSs in the network. The comparison of the proposed network with networks suggested in related works is presented in Figures 4.5 to 4.7.

Figure 4.5 represents the difference in average content delivery delay between the compared networks depending on the number of the FlyBSs in the network. The Figure shows that the average delay in delivering content in the compared networks decreases with the rise in the number of the FlyBSs. It is an expected outcome as the number of the FlyBSs in the network influences the available bandwidth for UEs, the same as the availability of cached contents. The Figure then shows that the average delivery delay is approximately 31% smaller in the proposed network than in the network suggested in [22] and approximately 39% smaller than in the network suggested in [15] for 3 FlyBSs in the network. The difference increases with the rise of the number of the FlyBSs, and for 6 FlyBSs in the network, the average delivery delay in the proposed network achieves values approximately 38% lower than in the network suggested in [22]. The comparison of the average delivery delay with the network suggested in [15] shows an increase of another 20%. The difference is caused by a better distribution of contents to the UEs in the proposed network, the same as by the lower load of communication left on the SBS.

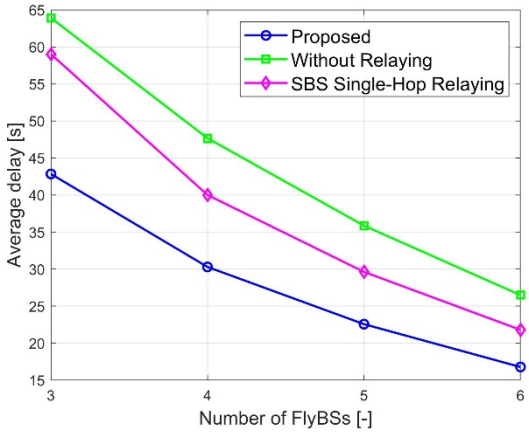

Figure 4.5 - Average content delivery delay depending on the number of FlyBSs in the network, Number of UEs K = 50, FlyBS's cache storage $s^{(BS)}$ = 3 Gbit

Figure 4.6 represents the difference in average content delivery delay between the compared networks depending on the number of the UEs in the network. The Figure displays the average content delivery delay rapidly increases with the number of the UEs in the network. It is caused by the distribution of constantly sized bandwidth between the rising number of the UEs in the network. The increased number of transmissions in the network then leads to intensified interference, which also negatively influences the capacity of channels. The average content delivery delay in the proposed network is the lowest from the compared networks for each number of the UEs in the network. The average content delivery delay difference then increases with the number of the UEs in the network., The average content delivery delay in the proposed network then achieves values approximately 28% lower than in the network suggested in [22] for 40 UEs in the network. The comparison of the average delivery delay with the network suggested in [15] shows an increase of another 6 %. The difference is caused by the improved distribution of communication resources to the UEs in the proposed network, the same as by the deployment of multi-hop relaying, which does not burden the overload bandwidth of the SBS. The improvement is also influenced by the FlyBS repositioning, which decreases the number of channels in the network.

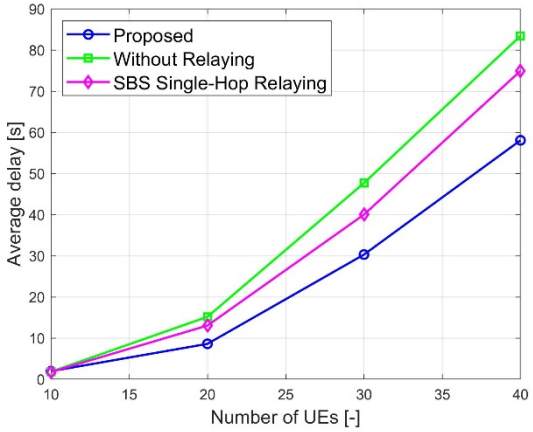

Figure 4.6 - Average content delivery delay depending on the number of UEs in the network, Number of FlyBSs U = 4, FlyBS's cache storage $s^{(BS)}$ = 3 Gbit

Figure 4.7 represents the difference in average content delivery delay between the compared networks depending on the storage size for caching of contents on the FlyBSs in the network. The Figure displays that the average content delivery delay decreases with the rise of cache storage size on the FlyBS in the case of each network. It is a result of the increased availability of cached contents close to the UEs, which decreases the network's total number

of active channels and thus increases the available bandwidth per channel on each BS. It is then possible to read from the Figure that the average content delivery delay in the proposed network is the smallest for each cache storage size in between compared networks. Compared to the network suggested in [22], the average content delivery delay in the proposed network is smaller by approximately 26 %. In contrast with the network suggested in [15], it is smaller by approximately 40%. The difference significantly influences the relaying enabled to originate from the FlyBSs in the proposed network, the same as multi-hop relaying and FlyBS repositioning, which frees up communication resources in the

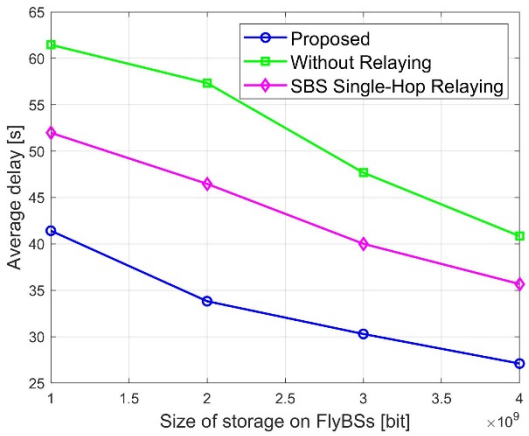

Figure 4.7 - Average content delivery delay depending on the size of cache storage on FlyBSs, Number of FlyBSs U = 4, Number of UEs K = 30

network.

5 Conclusions

This diploma thesis examined the possibility of content caching on FlyBSs and SBSs, and its possible cooperation to ensure the low energy consumed for communication in the network. This thesis proposes adjustments to the movement of FlyBSs, or improvements in how the contents are delivered to UEs presented in related works. Proposed mechanisms include the popularity-based content caching, the energy consumption navigated UE to BS association, and the content delivery through multi-hop relaying, modified by the FlyBS repositioning.

The simulation results show that the proposed network with proposed mechanisms significantly improves the energy consumed for communication in the network compared to related works. It also enhances the delay of content delivery. The energy consumed for communication decreases by approximately 27%-66% with respect to related works. The delivery delay is then, in comparison with related works, improved by 26%-58%. The gain depends on the number of FlyBSs and UEs in the network and on the size of cache storage on FlyBSs. The improvements have been achieved mainly thanks to the implementation of multi-hop relaying, which is enabled to originate from FlyBSs. A notable effect on the improvement also has the FlyBS repositioning in the content delivery.

This thesis aimed to find a UE association, power allocation, and FlyBS positioning in a mobile network, ensuring lower energy consumed for communication than in networks presented in related works examining the UAV-assisted mobile networks containing content caching. The simulation results prove that implementing the proposed mechanisms in mobile networks containing content caching and UAVs as FlyBSs improves the energy consumed for communication in the network. Thus, the purpose of this thesis was fulfilled.

The outcome of this thesis can be used for future research, which can extend the calculation of energy consumption by adding the propulsion power needed for the operation of UAVs. This addition would bring new knowledge about the energy consumption of UAV-assisted mobile networks.

References

[1] Y. Zeng, R. Zhang and T. J. Lim, "Wireless communications with unmanned aerial vehicles: opportunities and challenges," in *IEEE Communications Magazine*, vol. 54, no. 5, pp. 36-42, May 2016, doi: 10.1109/MCOM.2016.7470933.

[2] T. Zhang, Z. Wang, Y. Liu, W. Xu and A. Nallanathan, "Caching Placement and Resource Allocation for Cache-Enabling UAV NOMA Networks," in *IEEE Transactions on Vehicular Technology*, vol. 69, no. 11, pp. 12897-12911, Nov. 2020, doi: 10.1109/TVT.2020.3015578.

[3] T. Sap, *Deployment of Flying Base Stations in Emergency Situations.* Prague, 2022. Master thesis, Czech Technical University in Prague, Faculty of Electrical Engineering, Department of Telecommunications Engineering. Supervisor doc. Ing. Z. Bečvář, Ph.D.

[4] Y. Zeng, R. Zhang and T. J. Lim, "Throughput Maximization for UAV-Enabled Mobile Relaying Systems," in *IEEE Transactions on Communications*, vol. 64, no. 12, pp. 4983-4996, Dec. 2016, doi: 10.1109/TCOMM.2016.2611512.

[5] S. Zhang, H. Zhang, Q. He, K. Bian and L. Song, "Joint Trajectory and Power Optimization for UAV Relay Networks," in *IEEE Communications Letters*, vol. 22, no. 1, pp. 161-164, Jan. 2018, doi: 10.1109/LCOMM.2017.2763135.

[6] F. Cheng, G. Gui, N. Zhao, Y. Chen, J. Tang and H. Sari, "UAV-Relaying-Assisted Secure Transmission With Caching," in *IEEE Transactions on Communications*, vol. 67, no. 5, pp. 3140-3153, May 2019, doi: 10.1109/TCOMM.2019.2895088.

[7] Y. Chen, W. Feng and G. Zheng, "Optimum Placement of UAV as Relays," in IEEE Communications Letters, vol. 22, no. 2, pp. 248-251, Feb. 2018, doi: 10.1109/LCOMM.2017.2776215.

[8] Q. Tang, L. Liu, C. Jin, J. Wang, Z. Liao and Y. Luo, “An UAV-assisted mobile edge computing offloading strategy for minimizing energy consumption,” in *Computer Networks*. 2022, 207. ISSN 13891286. doi:10.1016/j.comnet.2022.108857

[9] G. I. P. Association et al., “5G vision-the 5G infrastructure public private partnership: The next generation of communication networks and services,” White Paper, Feb. 2015.

[10] J. Yang, S. Xiao, B. Jiang, H. Song, S. Khan and S. u. Islam, "Cache-Enabled Unmanned Aerial Vehicles for Cooperative Cognitive Radio Networks," in *IEEE Wireless Communications*, vol. 27, no. 2, pp. 155-161, April 2020, doi: 10.1109/MWC.001.1900301.

[11] M. Zhang, M. EI-Hajjar and S. X. Ng, "Intelligent Caching in UAV-Aided Networks," in *IEEE Transactions on Vehicular Technology*, vol. 71, no. 1, pp. 739-752, Jan. 2022, doi: 10.1109/TVT.2021.3125396.

[12] M. G. Khoshkholgh, K. Navaie, H. Yanikomeroglu, V. C. M. Leung and K. G. Shin, "Randomized Caching in Cooperative UAV-Enabled Fog-RAN," 2019 *IEEE Wireless Communications and Networking Conference (WCNC)*, 2019, pp. 1-6, doi: 10.1109/WCNC.2019.8885486.

[13] J. Ji, K. Zhu, D. Niyato and R. Wang, "Joint Cache Placement, Flight Trajectory, and Transmission Power Optimization for Multi-UAV Assisted Wireless Networks," in *IEEE Transactions on Wireless Communications*, vol. 19, no. 8, pp. 5389-5403, Aug. 2020, doi: 10.1109/TWC.2020.2992926.

[14] D. -H. Tran, S. Chatzinotas and B. Ottersten, "Throughput Maximization for Backscatter- and Cache-Assisted Wireless Powered UAV Technology," in *IEEE Transactions on Vehicular Technology*, vol. 71, no. 5, pp. 5187-5202, May 2022, doi: 10.1109/TVT.2022.3155190.

[15] A. A. Khuwaja, Y. Zhu, G. Zheng, Y. Chen and W. Liu, "Performance Analysis of Hybrid UAV Networks for Probabilistic Content Caching," in *IEEE Systems Journal*, vol. 15, no. 3, pp. 4013-4024, Sept. 2021, doi: 10.1109/JSYST.2020.3013786.

[16] A. Al-Hourani, S. Kandeepan and S. Lardner, "Optimal LAP Altitude for Maximum Coverage," in *IEEE Wireless Communications Letters*, vol. 3, no. 6, pp. 569-572, Dec. 2014, doi: 10.1109/LWC.2014.2342736.

[17] M. Nikooroo and Z. Becvar, "Optimal Positioning of Flying Base Stations and Transmission Power Allocation in NOMA Networks," in *IEEE Transactions on Wireless Communications*, vol. 21, no. 2, pp. 1319-1334, Feb. 2022, doi: 10.1109/TWC.2021.3103639.

[18] Y. Zeng, J. Xu and R. Zhang, "Energy Minimization for Wireless Communication With Rotary-Wing UAV," in *IEEE Transactions on Wireless Communications*, vol. 18, no. 4, pp. 2329-2345, April 2019, doi: 10.1109/TWC.2019.2902559.

[19] N. Hu, X. Qin, N. Ma, Y. Liu, Y. Yao and P. Zhang, "Energy-efficient Caching and Task offloading for Timely Status Updates in UAV-assisted VANETs," *2022 IEEE/CIC International Conference on Communications in China (ICCC)*, 2022, pp. 1032-1037, doi: 10.1109/ICCC55456.2022.9880683.

[20] P. Mach, Z. Becvar and M. Najla, "Joint Association, Transmission Power Allocation and Positioning of Flying Base Stations Considering Limited Backhaul," *2020 IEEE 92nd Vehicular Technology Conference (VTC2020-Fall)*, 2020, pp. 1-7, doi: 10.1109/VTC2020-Fall49728.2020.9348784.

[21] O. Durmaz Incel and P. Jansen, "Characterization of multi-channel interference," in *6th International Symposium on Modeling and Optimization in Mobile, Ad Hoc, and Wireless Networks and Workshops*, 2008, pp. 429-435, doi: 10.1109/WIOPT.2008.4586102.

[22] J. Luo, J. Song, F. -C. Zheng, L. Gao and T. Wang, "User-Centric UAV Deployment and Content Placement in Cache-Enabled Multi-UAV Networks," in *IEEE Transactions on Vehicular Technology*, vol. 71, no. 5, pp. 5656-5660, May 2022, doi: 10.1109/TVT.2022.3152246.